THE INFLUENCE OF PEPTIDE FUNCTIONALIZED GOLD NANOPARTICLES ON PROSTATE CANCER CELLS

by
Merve Ercan

Submitted to Graduate School of Natural and Applied Sciences
in Partial Fulfillment of the Requirements
for the Degree of Master of Science in
Biotechnology

Yeditepe University
2018

THE INFLUENCE OF PEPTIDE FUNCTIONALIZED GOLD NANOPARTICLES ON PROSTATE CANCER CELLS

APPROVED BY:

Prof. Dr. Mustafa Çulha
(Thesis Supervisor) .....

Assoc. Prof. Dr. Kaan Keçeci .....

Assist. Prof. Dr. Andrew John Harvey .....

DATE OF APPROVAL: ..../..../2018

ACKNOWLEDGEMENTS

First I would like to express my gratitude to my advisor Prof. Mustafa Çulha who is the one always successfully being both teacher and manager. I thank to him for giving me the chance to work with him, and being always pillar of support. I have valuable quotes from him that I am going to keep in my lifesaver bag till the end.

I would like to thank all the members of Nanobiotechnology Research Group for their debonairness and helpfulness since the beginning. I especially thank to Dr. Gamze Kuku who is always supportive and calming to me. I thank you all very very much from my heart for being always sweet-natured and sisterly Zehra Çobandede, Dr. Seda Keleştemur, Dr. Sevda Mert, Zeynep Işık, Hande Duru Köktaş, Dr. Mine Altunbek, and to my honey bunny mate Deniz Uzunoğlu. The other very especial thank goes to my labmate Melike Sarıçam whom I learned so much from.

I am thankful to my roomie Suzan Alınlı so much for always encouraging me, and being there for eating and dancing whether it be 2 am or 2 pm, and not killing me when I am being intentionally annoying her. I also thank to my short term roomie the great pychologist candidate Şeyma Saçan for her insight and good humour.

I am deeply thankful to Hazal Özlem Ersan Eruş and Turkish Chemical Society for being good reasons to keep my aspire to be a scientist.

I thank to my family Ö.Muzaffer, Hatice, Emre, Kübra for their love and support. I would like to a very special thank to my dear lovely niece N.Duru Ercan. Last but not least I thank to Y.Can Ayra for always being there, and making the bad stuff bearable and the good things more beautiful.

ABSTRACT

THE INFLUENCE OF PEPTIDE FUNCTIONALIZED GOLD NANOPARTICLES ON PROSTATE CANCER CELLS

Nanomaterials have emerged as new tools for theranostic applications. However, their use in biomedical fields is limited by their potential toxic effects on human health. It has been indicated in the literature that functionalizing the surface of NPs is a favorable approach to eliminate the safety issue of the nanomaterials. AuNPs provide a platform for designing therapeutic biomaterials owing to their easy surface chemistry, less toxicity, biocompatibility, high degree of stability and size uniformity. Besides, small differences in the surface chemistry of AuNPs can be observed by UV/Vis spectroscopy due to their unique plasmonic properties. Functionalization of AuNPs with a small biomolecule introduces a good platform to enhance cellular uptake and reduce the toxicity. In this study, a range of custom designed peptides were choosen for modification of the 13 nm AuNPs by taking their sequence, size, and charge into account. To evaluate cellular responses comparatively, both healthy (PNT1A) and cancer (DU145) cell lines were treated with the AuNP-Peptide conjugates. The peptide modified AuNPs indicated more toxic effects on DU145 cells than PNT1A cells, and the position of Cys amino acid in the sequence caused difference in cytotoxicity. Furthermore, the AuNP-Peptides induced the apoptotic cell death in prostate cancer cells in contrast to response of healthy cells. Pep1 (H_2N-Glu-Glu-Glu-Cys-COOH) and Pep5 (H_2N-Asp-Gly-Arg-Glu-Glu-Glu-Cys-COOH) modified AuNPs significantly induced apoptotic cell death for DU145 cell line compared to Cys-N-terminal peptide modified AuNPs. In addition, the cell cycle of the PNT1A and DU145 cells were also investigated. While the DU145 cells were arrested at G2/M phase in a high ratio, there was no significant arrest for PNT1A cells. The highest arrest in G0/G1 phase of the PNT1A cells obtained with the His containing Cys-C-terminal peptide. In conclusion, it was shown that subtle changes in surface chemistry of AuNPs caused noticeable difference in cellular response, which indicates the importance of tailoring surface chemistry of nanomaterials aimed to be used in nanomedicine.

ÖZET

PEPTİTLE FONKSİYONELLEŞTİRİLMİŞ ALTIN NANOPARÇACIKLARIN PROSTAT KANSERİ HÜCRELERİNE ETKİSİ

Nanomalzemeler, terapötik uygulamalar için yeni araçlar olarak ortaya çıkmışlardır. Bununla birlikte, biyomedikal alanlardaki kullanımları, insan sağlığı üzerindeki potansiyel toksik etkileri nedeniyle sınırlıdır. Literatürde, NP'lerin yüzeyini işlevsel hale getirmenin, nanomalzemelerin güvenlik problemini ortadan kaldırmak için uygun bir yaklaşım olduğu belirtilmiştir. AuNP'ler, kolay yüzey kimyaları, düşük toksisiteleri, biyo-uyumlulukları, yüksek stabiliteleri ve boyut üniformiteleri sayesinde terapötik biyomateryallerin tasarlanması için elverişli bir platform sağlarlar. Ayrıca, AuNP'lerin yüzey kimyalarındaki küçük farklılıklar, eşsiz plazmonik özellikleri sayesinde UV/GB spektroskopisi ile gözlemlenebilir. AuNP'lerin küçük biyomoleküller ile fonksiyonel hale getirilmesi, hücresel alımı arttırma ve toksisiteyi azaltma konusunda iyi bir çözüm sunar. Bu çalışmada 13 nm AuNP'lerin modifikasyonu için; dizilimleri, uzunlukları ve yükleri dikkate alınarak çeşitli peptitler seçilmiştir. Hücresel cevabı karşılaştırmalı değerlendirmek için, sağlıklı (PNT1A) ve kanser (DU145) hücre dizilerinin her ikisi de AuNP-Peptit konjugeleri ile muamele edilmiştir. Peptit modifiye AuNP'ler, DU145 hücreleri üzerinde PNT1A hücrelerinde gösterdiğinden daha fazla sitotoksik etki göstermiştir ve Cys amino asidinin pozisyonunun sitotoksik etkide fark yarattığı görülmüştür. Bununla birlikte, AuNP-Peptitler sağlıklı hücrelerde gözlenenin aksine, prostat kanseri hücrelerinde apoptotik hücre ölümüne neden olmuşlardır. Pep1 (H_2N-Glu-Glu-Glu-Cys-COOH) ve Pep5 (H_2N-Asp-Gly-Arg-Glu-Glu-Glu-Cys-COOH) modifiye AuNP'ler, Cys-N-terminal peptit modifiye AuNP'lere kıyasla DU145 hücre hattında açık bir farkla apoptotik hücre ölümüne sebep olmuşlardır. Ek olarak, PNT1A ve DU145 hücrelerinin hücre döngüsü de araştırılmıştır. DU145 hücreleri yüksek oranda G2/M fazında tutulurken, PNT1A hücreleri için önemli bir duraklamaya rastlanmamıştır. En yüksek G0/G1 fazında tutulma oranı His amino asidi içeren Cys-C-terminal peptit ile PNT1A hücre hattında görülmüştür. AuNP yüzeyindeki küçük değişimlerin hücresel yanıtta önemli farklılıklara sebep olduğu, böylece yüzey kimyası terziliğinin nanotıp alanında kullanımının önemi gösterilmiştir.

TABLE OF CONTENTS

ACKNOWLEDGEMENTS iii

ABSTRACT iv

ÖZET v

LIST OF FIGURES viii

LIST OF TABLES x

LIST OF SYMBOLS/ABBREVIATIONS xi

1. THEORETICAL BACKGROUND 1

1.1. NANOTECHNOLOGY 1

1.2. NANOPARTICLES IN BIOTECHNOLOGY 1

1.2.1. Gold Nanoparticles and Their Applications in Biotechnology and Medicine 3

1.2.2. Surface Modification of Gold Nanoparticles 5

1.2.3. Common Methods for Surface Modification of Gold Nanoparticles 6

1.2.4. Peptide Modified Gold Nanoparticles 9

1.3. PROSTATE CANCER 10

1.3.1. Diagnosis and Therapy Approaches for Prostate Cancer 11

1.3.2. Nanotechnology in Diagnosis and Therapy of Prostate Cancer 11

2. AIM OF THE STUDY 13

3. MATERIALS 14

3.1. CHEMICALS AND KITS 14

3.1.1. AuNPs 14

3.1.2. Peptides 14

3.1.3. Cell Culture Reagents and Kits 16

3.2. CELL LINES 16

3.3. INSTRUMENTS 16

4. METHODS 17

4.1. SYNTHESIS OF GOLD NANOPARTICLES 17

4.2. MODIFICATION OF GOLD NANOPARTICLES WITH THE PEPTIDES 17

4.3. CHARACTERIZATION OF THE GOLD NANOPARTICLES AND GOLD NANOPARTICLES WITH THE PEPTIDES 17
4.3.1. UV/Vis Spectroscopy 18
4.3.2. Dynamic Light Scattering 18
4.3.3. Transmission Electron Microscopy Analysis 18
4.3.4. Fourier Transmission Infrared (FTIR) Spectroscopy Analysis 18
4.3.5. Agarose Gel Electrophoresis 19
4.4. CELL CULTURE 19
4.5. TREATMENT OF THE CELLS WITH THE PEPTIDE FUNCTIONALIZED GOLD NANOPARTICLES 19
4.6. APOPTOSIS/NECROSIS ASSAY 19
4.7. WST-1 CELL PROLIFERATION ASSAY 20
4.8. CELL CYCLE ANALYSIS 20
5. RESULTS AND DISCUSSION 22
5.1. CHARACTERIZATION OF THE GOLD NANOPARTICLES AND THE GOLD NANOPARTICLES WITH THE PEPTIDES 22
5.1.1. AuNPs 22
5.1.2. Peptide Modified AuNPs 23
5.1.2.1. Behaviour of the AuNP-Peptide Conjugates in Aqueous Media 25
5.1.2.2. UV/Vis Spectroscopy 30
5.1.2.3. Dynamic Light Scattering 31
5.1.2.4. Agarose Gel Electrophoresis 32
5.1.2.5. Fourier Transform Infrared Spectroscopy 33
5.2. EFFECT OF THE AuNP-PEPTIDES ON PROSTATE CANCER CELLS 34
5.2.1. Cytotoxicity 34
5.2.1.1. WST-1 Cell Proliferation Assay 35
5.2.1.2. Apoptosis-Necrosis Assay 37
5.2.2. Cell Cycle 40
6. CONCLUSION AND FUTURE PERSPECTIVE 43
REFERENCES 45

LIST OF FIGURES

Figure 1.1. Schematic representation of nanoscale in comparison (20). 2

Figure 1.2. TEM images of the different shapes of gold nanoparticles (45). 4

Figure 1.3. Representative interactions between the biomolecule and gold nanoparticles (a) covalent (b) hydrophobic (c) ionic (99). 7

Figure 1.4. Conjugation of citrate capped gold nanoparticle with the biomolecule by EDC/NHS coupling (78). 8

Figure 1.5. The prostate diagram (119). 10

Figure 3.1. Molecular structures of the peptides. 15

Figure 5.1. The image of the 13 nm AuNP suspension. 22

Figure 5.2. A) UV/Vis B) DLS spectrum of the synthesized AuNPs. 23

Figure 5.3. TEM image of the 13 nm AuNPs. 23

Figure 5.4. Images of the AuNP suspensions before and after peptide addition. 25

Figure 5.5. The AuNPs suspensions at various pH in range of 3-12. 26

Figure 5.6. The AuNP-Peptide suspensions. 27

Figure 5.7. Schematical representation of the AuNP-Peptide bioconjugation reactions. 29

Figure 5.8. UV/Vis spectra of AuNPs and AuNP-Peptides suspensions 30

Figure 5.9. DLS spectra of AuNPs and AuNP-Peptides suspensions. 31

Figure 5.10. Image of the 1 per cent agarose gel electrophoresis result of the peptide modified AuNPs. 33

Figure 5.11. FT-IR spectra of the bare AuNPs and the AuNP-Peptide conjugates. 34

Figure 5.12. Reduction of the tetrazolium salt to formazan. 35

Figure 5.13. Cell viability of (a) PNT1A (b) DU145 cells at increasing concentrations of the AuNPs and the AuNP-Peptides. 36

Figure 5.14. Apoptosis-necrosis analysis of PNT1A cells. 38

Figure 5.15. Apoptosis-necrosis analysis of DU145 cells. 39

Figure 5.16. The cell cycle analysis of the AuNP-Peptide exposured PNT1A cells. 41

Figure 5.17. The cell cycle analysis of the AuNP-Peptide exposured DU145 cells.....42

LIST OF TABLES

Table 3.1. The sequences, molecular weights, isoelectric points and charges of the peptides used to modify the surfaces of 13 nm AuNPs. 14

Table 5.1. The sequences, isoelectric points, and charges of the peptides used to modify the surfaces of 13 nm AuNPs. 24

Table 5.2. The peptides sequences and the needed pH conditions for the stabile AuNP-peptides in aqueous media. 27

Table 5.3. Needed pH values for the AuNP-Peptide conjugation reactions. 28

Table 5.4. Average diameter and zeta potential values of the AuNPs and the AuNP-Peptide conjugates. 32

LIST OF SYMBOLS/ABBREVIATIONS

cm	Centimeter
cm^{-1}	Wavenumber
d.nm	Diameter in nanometer scale
g	Gram
h	Hour
mg	Miligram
min	Minute
ml	Mililiter
mM	Milimolar
mW	Miliwatt
nM	Nanomolar
nm	Nanometer
ºC	Degrees Celsius
rpm	Rounds per minute
V	Volt
µl	Microliter
µM	Micromolar
λ	Wavelength
Ω	Electrical resistance
AGE	Agarose gel electrophoresis
AgNPs	Silver nanoparticles
Arg	Arginine
Asp	Asparagine
AuNP-Pep	Peptide functionalized gold nanoparticle
AuNPs	Gold nanoparticles
$C_6H_5Na_3O_7.2H_20$	Trisodium citrate dihydrate
CNT	Carbon nanotube
Cys	Cysteine

DLS	Dynamic light scattering
DMEM	Dulbecco's modified Eagle's medium
DNA	Deoxyribonucleic acid
EDC	1-Ethyl-3-(3-dimethylaminopropyl)-carbodiimide
EDTA	Ethylenediaminetetraacetic acid
EGCG	Epigallocatechin gallate
EGFR	Epidermal growth factor receptor
FBS	Fetal bovine serum
FTIC	Fluorescein isothiocyanate
FTIR	Fourier transmission infrared
Glu	Glutaraldehyde
Gly	Glycine
GNPs	Gold nanoparticles
$HAuCl_4.3H_2O$	Tetrachloro auric acid trihydrate
HCl	Hydrochloric acid
HER2	Human epidermal growth factor receptor
His	Histidine
ICP-MS	Inductively coupled plasma-mass spectrometer
IR	Infrared
LOD	Limit of detection
M_w	Molecular weight
MWCNT	Multi-walled carbon nanotube
NaOH	Sodium hydroxide
NHS	N-hydroxysuccinimide
NMs	Nanomaterials
NPs	Nanoparticles
PBS	Phosphate buffered saline
PEG	Poly(ethylene glycol)
pI	Isoelectric point
PI	Propidium Iodide
PLGA	Poly(lactic-co-glycolic acid)
PS	Penicilin streptomycin
PSA	Prostate specific antigen

PSMA	Prostate specific membrane antigen
QDs	Quantum dots
RGD	Arginine-glycine-aspartic acid
RNA	Ribonucleic acid
SEM	Scanning electron microscopy
SERS	Surface enhanced Raman scattering
SPR	Surface plasmon resonance
TAE	Trizma base-acetic acid-ethylenediaminetetraacetic acid
TEM	Transmission electron microscopy
UV/Vis	Ultraviolet/Visible
WST-1	Water-soluble tetrazolium-1

1. THEORETICAL BACKGROUND

1.1. NANOTECHNOLOGY

Nanotechnology is quite a part of our life for many years by involving many application fields such as coating technologies [1], clean water supplying [2], defense industry [3], textiles [4], antibacterial production [5], food packaging [6], controlled drug delivery and targeting systems [7], gene silencing [8]. Also, nanotechnology is the main character of the nano-smart technologies and nanocomposite materials owing to their unique optoelectronic and fluorescence features [9, 10]. Further, nanotechnology has been continuing to grow, and promising for the future in many of vital fields such as medicine and bioimaging [11–14], drug and gen delivery [15], vaccine development [16], biosensors, and therapies [7–11]. The point, which makes nanotechnology a favorable study field is physically and chemically quite different behavior of the materials when they are nano-sized in order to bulk or large-scale. In other words as Chad Mirkin says; "*everything, when miniaturized to the sub-100-nanometer scale, has new properties, regardless of what it is*" [17]. The acquisition of unique properties in nano-scale is explained by surface to volume ratio (S/V) refering to the surface area divided by the volume of the material. For instance, this ratio is inversely proportional to edges of a cube. Thus, as the S/V increases with the number of particles (molecules/atoms) are present in a smaller specific area, which means forming of "dangling bonds" on the surface of the material and higher chemical activity. In this way, high electrical and chemical activities of the nano-sized materials and unique catalytic properties of noble metals such as Au and Pt, can be clarified with this "the less surface the more energy" behavior [18]. Likewise graphene is taken into account, it has large number of unsaturated bonds on its surface resulting in high S/V ratio, which makes it significantly convenient for sensor applications [19].

1.2. NANOPARTICLES IN BIOTECHNOLOGY

"Nano" as a term of measurement is meaning billionth of a meter. Materials having size in the range of 1 to 100 nanometers in at least one dimension are called as "nanomaterials".

Thus the new research areas arised with “nano” term such as nanomedicine, nanobiotechnology, and nanoelectronics.

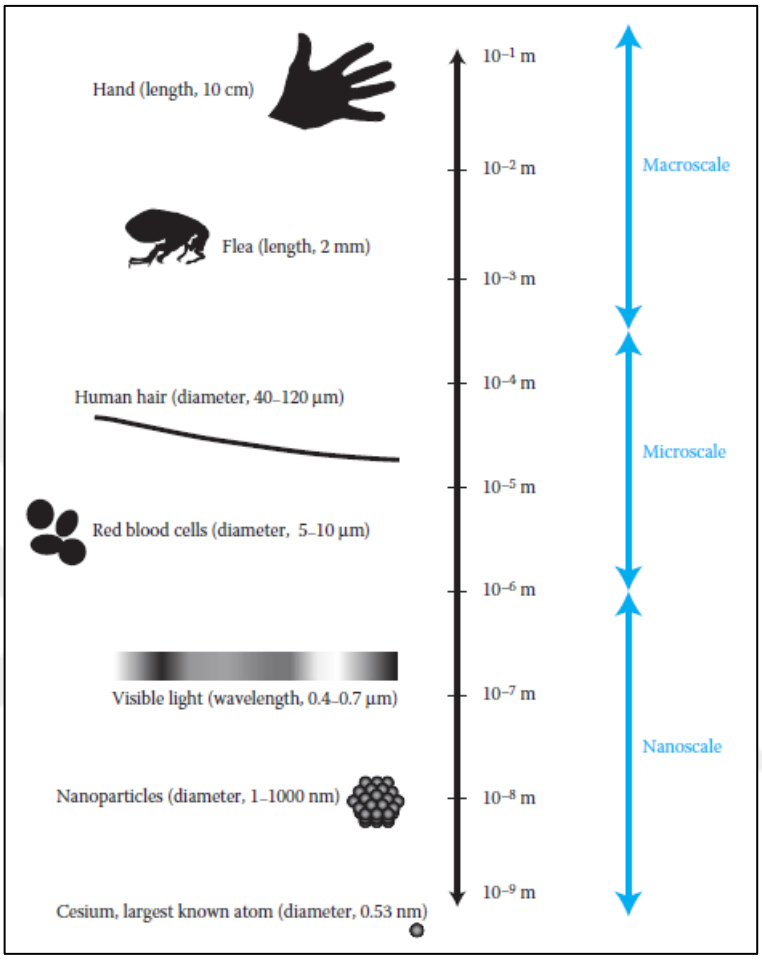

Figure 1.1. Shematic representation of nanoscale in comparison [20].

The nanomaterials having biocompatibility promise for many medical applications. Among them, carbon nanotubes (CNTs), quantum dots (QDs) [21], silver nanoparticles (AgNPs) and gold nanoparticles (AuNPs) have quite importance in medical fields according to their relatively stability in biological media, low toxicity and novel optical properties which are providing detection specific molecules and imagining by spectroscopic and microscopic techniques.

- CNTs have attracted great interest in sensor, composite material, nano-device technologies [22–24] owing to their convenient mechanical, electronic, magnetic and optical features [25–27]. Also, they are quite strong materials due to their C-C

bonds, and have good viscoelastic properties which can provide hosting as soft tissue membranes [28].

- QDs have a place in live cell imaging and diagnostics due to their characteristic photochemical properties [29]. Also their fluorescent emission wavelength can be tunable by altering their size. They able to be used instead of organic dyes of fluorescent proteins due to their relatively high stability, and they are brighter than dyes [30, 31]. Besides their potential use in many biotechnological applications such as immunosensors, DNA array analysis, and cell biology, they can be designed to be multifunctional. Additionaly, their another distict feature is that small amount of QDs is needed for a signal [32].
- AgNPs have a significant importance in many research area due to their plasmonic and antibacterial properties, which are tunable by altering their size and shape. In this way, the researchers have been focused on uniform synthesis of AgNPs in a variety of shapes [33, 34]. The common two methods for synthesis of AgNPs is citrate and sodium borohydride reduction [35, 36]. Additionally, they have been used as surface enhanced Raman scattering (SERS) substrates owing to their unique plasmonic properties [37].

1.2.1. Gold Nanoparticles and Their Applications in Biotechnology and Medicine

The use of soluble gold began in around 5th century B.C. in Egypt and China for glass staining [38]. Then, its potential use in medicine was investigated by Francis Anthony. Following these approaches on gold, Faraday leaded for use of AuNPs in today's high-tech applications by investigated their optical properties in 18th century. He produced the first colloidal gold solution. Many features of colloidal gold have been clarified up to day, and it has found place in several study fields. Also controllable easy synthesis in various sizes, easy surface modification, biocompatibilty and chemically stability are the other features that make them favourable. There are several methods for the synthesis of AuNPs [39–43]. Among them, Turkevich method based on reduction of choloroauric acid by trisodium citrate [44] is most preferred because of providing monodisperse size distiribution, high stability in aqueous media and tunable size. Also, they able to be synthesized in various shapes as rod, triangular, or cube which indicate different optical and magnetic features (Figure 1.2).

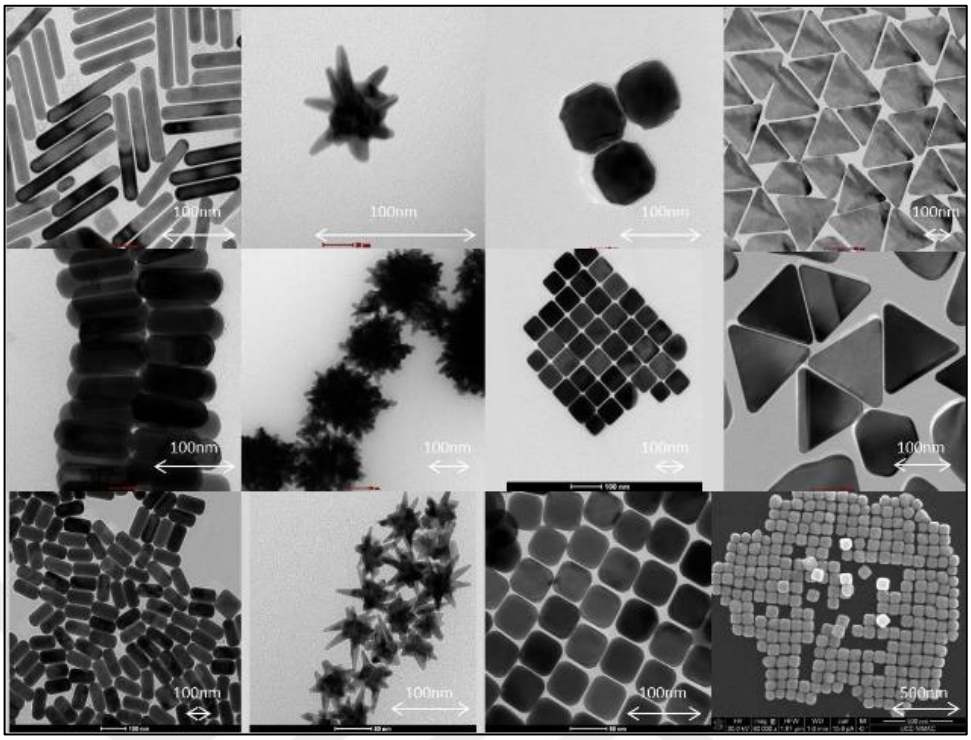

Figure 1.2. TEM images of the different shapes of gold nanoparticles [45].

In recent years, AuNPs were attractive for researchers due to their feasibility for such crucial study fields as electronics [46], biomedicine [47], drug delivery and bioimaging [48], surface functionalization [49–52] and sensing [53]. Their surface plasmon formation due to their interaction with visible light [54, 55] makes them convenient to the use for electronic devices, signal amplification, and biosensing platforms based upon colorimetry [56], flourescence [57, 58], electrochemistry [59], surface plasmon resonance (SPR), surface enhanced Raman scattering (SERS) [53, 60]. They are used in photothermal therapy; the gold nanorods are applied to tumor and heated by IR radiation [61]. Thus, AuNPs have a curicial place in medical research. For instance, DNA sensor was developed by taking advantage of the colorimetric change based on their plasmonic features [62, 63], and in the light of this approach other biological targets were studied such as peptides, oligonucleotides and cells [64–67]. On the other hand, the use of AuNPs in theranostic applications faces with some challenges such as cellular uptake and stability in body fluids. Toxicity is another issue for AuNPs due to their interaction with human body. Their cell penetration and stability in body fluids are also needed to be improved.

1.2.2. Surface Modification of Gold Nanoparticles

Nanoparticles can affect the fate of living cells, designate their pathway and modulate their death [68-71]. The new approaches to synthesize novel nanobiostructures are lead to engender therapeutic agents for cancer treatment. Amphiphilic properties of cell memrane enable to cellular uptake and provide a wide range of small biological molecules. Thus, it is possible to develop nanoparticles modified with biological materials for both easy cellular uptake and theraphy. Before the penetrating of the nanomaterial in cell, they interact with the environment of the cell which affects on the biological properties of the nanostructure and intracellular pathway. Another issue is prone to agglomeration of these small particles. Upon this, the efficient size of the nanomaterial for cellular uptake and targeting is affected. Thus, it is comprehended that the aspects that needed to be improved are their cell penetration, stability in body fluids, and less cytotoxicity. Eliminating this issue is achieved by providing the hydrophobicity balance between NMs and cell membrane, stability of the NMs in biological media, and controlling biodistribution of them, which are possible by coating the NP with variety of biomolecules named as “surface engineering/modification” [32, 72]. Because these mechanisms are directly related with the chemical characteristics, morphology, and surface properties of the NMs [73]. Upon this, they can be modified with various molecules, that provide affinity force between molecules, including peptides [74, 75], proteins [76], carbohydrates [77], fatty acids, DNA [78], plasmids, and RNA [79–82]. At this point, the bioconjugation approach arises, and here the key point is not causing to lose the activity of the NPs, while altering their surface chemistry. In this respect, the modification agent and the method have crucial places separately. The method is chosen in consideration of the substrate, and the molecular interactions between the substrate and surface of the NPs. The substrate is relating with the producing purpose of the NMs. Thus, the NMs can be enabled for a variety of medical application areas such as biosensing, bioimaging, controlled drug delivery, therapy, and diagnostics [43, 83–85].

Gold nanoparticles are commonly modified with thiols, citrate, surfactants, polymers, carbohydrates, hormones, and lipids [86, 87]. Among them, amino acids and sulphydryl groups are more favourable owing to their small size, low steric hindrance, and easy conjugation to the AuNPs. These groups serve as stabilizator and/or functioning agent. The

stabilization of the NPs can be carried out with a macro-molecule as a polymer or a charged ligands (i.e. $-COO^-$, $-NH_3^+$), which can not only stabilize the NPs but also gain functionality for bioconjugation or ligand-exchange to them. The charged groups immobilized on the surface of the NPs change the electronic and binding features of the NMs. Thus, it can be tunable that stability, aggregation, solubility, electron transfer capability, size and shape features of the NMs [39, 43].

Modification of citrate capped AuNPs is relatively feasible owing to the weak interaction between AuNP and citrate group [88]. Thus, it can be easily exchanged with thiolated molecules, and thiol act as a linker between AuNP and variety of functional molecules such as polyethylene glycol (PEG) [89, 90], fluorescing dyes [91], and drugs [25]. GNPs capped using thiol chemistry have been widely studied with a range of therapeutic applications, including drug delivery and medical imaging [92, 93]. Altering the surface chemistry of GNPs using thiol have been widely studied with a range of therapeutic applications, including drug delivery and medical imaging [92, 93].

1.2.3. Common Methods for Surface Modification of Gold Nanoparticles

The interactions between the biomolecules and surface of AuNP are clarified in two approaches: as physically and chemically. Physical interactions are obtained as ionic, hydrophobic, and dative. As regards to chemical interactions, three ways are occurred: (i) chemisorption, (ii) via a linker molecule (iii) via an adapter molecule (Table 1.1) [94] .

Table 1.1. Interactions between the gold nanoparticles surface and the modification agents.

Physical Interactions	Ionic Interactions	Non-covalent
	Hydrophobic Interactions	
	Dative Binding	Covalent
Chemical Interactions	Chemisorption	
	Linkers	

	Adapter Molecules	

In other words, the biomolecule can be bonded onto the surface of AuNP as covalent or non-covalent [95]. Herein it is possible for the non-covalent bonding both hydrophobic and electrostatic interactions between the citrate capped AuNPs and the positively charged biomolecules [96]. Also the hydrophobic interaction occurs via hydrophobic side of the modification molecule and the AuNP surface. By virtue of this electrostatic interaction mechanism, attachment was provided between Human EGF Receptor 2 (HER2) specific antibody and AuNPs. Thus, detection of breast cancer cells was obtained by optical imaging with this nano-bio material [96]. In other study, 5-aminolevulinic acid and AuNPs conjugation was carried out by non-covalent binding to benefit for photodynamic therapy [97]. It was also applied for another cancer diagnosis application by binding of anti-EGFR to AuNPs non-covalently [98].

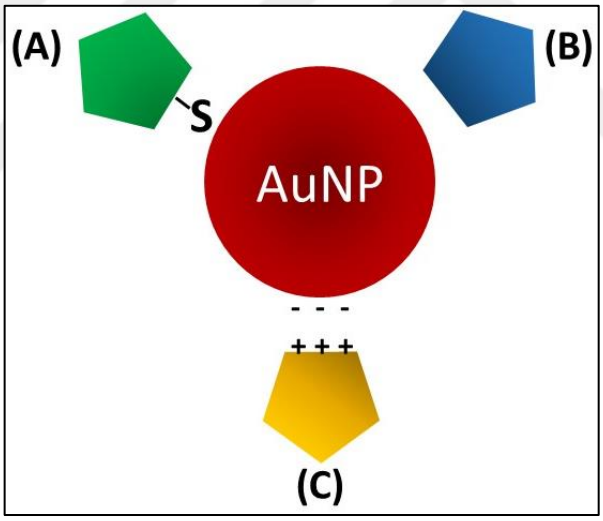

Figure 1.3. Representative interactions between the biomolecule and gold nanoparticles (a) covalent (b) hydrophobic (c) ionic [99].

On the other hand, non-covalent bonding has some drawbacks such as needed to be concentrated biomolecule-AuNPs samples, and instability of the bonds causing by their electrostatic attraction. Thus, the biomolecules on the surface of the NPs able to be exchanged with other small molecules. Besides, AuNPs can be modified by covalent bonding [95, 100]. Additionally, AuNPs able to be modified by thiol (-SH) included biomolecules owing to their tendency to thiol group. Upon this, the dative bonding is obtained by the interactions between AuNP surface and thiol groups, which is a type of

covalent bonding [101, 102]. Thus the covalently bonding is also available for NPs surface modification by the biomolecules. This attachment is occurred w/wo a linker or a spacer molecule such as avidin and biotin [95].

For the bioconjugation, it must be considered that when the NPs in a solution their stability may be affected by the environment. At this point, the way of the conjugation has a significant importance, and there are several functional groups to overcome this issue. For instance, carboxyl groups react with primary amines. Here, -COOH containing intermediate product is engendered by using a water soluble agent (i.e. EDC). Subsequently, suggested the primary amines existing on the NP surface, an active ester group (i.e. NHS) can be used for amide bonds [82, 103].

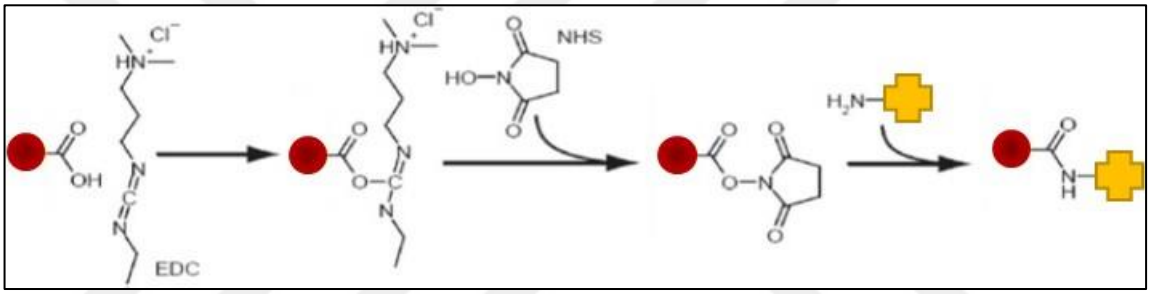

Figure 1.4. Conjugation of citrate capped gold nanoparticle with the biomolecule by EDC/NHS coupling [78].

Also the AuNPs are capped with PEG-SH to provide more hydrophilic character, and prevent undesirable reactions. In addition to this, PEG group provides a base for efficient covalent bonding, and capable to be modified with another molecule as a spacer.

The efficient interaction between –SH group and AuNP is a good platform for tailoring the surface of the AuNPs. It was used for conjugation of multiwall carbon nanotube (MWCNT) ionic liquid electrode and AuNPs, which serves as immunosensor for detection of human serum albumin in body fluids with low limit of detection (LOD) [104]. In another study, NHS-activated PEG was attached to an amine containing antibody. Subsequently, the structure was bonded to surface of AuNP nanocage resulting in the breaking of S-S bonds and creating of Au-S bonds [105]. Here EDC acts as a linker molecule between the AuNP and modification agent, and the covalent bond is provided by peptide bonds between N-terminal of the protein and –COOH groups on the AuNPs

causing by EDC [106, 107]. Also, nucleic acid-AuNPs interaction was obtained by thiolation of the AuNPs and adjusting convenient pH value to provide needed repulsion between the oligonucleotides and AuNP surface [108].

1.2.4. Peptide Modified Gold Nanoparticles

To provide self-assembling of the nanoparticles, they have been modified with various biomolecule such as DNA, viruses, proteins, and peptides. The resulting hybrid structures may not be strong enough through weak non-covalent interactions. Among these bio-modification agents, peptides are the most feasible due to their controllable chemical features by amino acid sequencing, capable to link ionic bonds, self-assembled characteristics [83, 109]. Peptides can bind directly to the AuNP surface through thiol group of cysteine amino acid or N terminal primary amine. Additionally, their biocompatibility make them favourable in medical applications such as drug delivery systems [43, 110, 111].

Preparing of the AuNP-Peptide conjugates is mostly obtained as synthesis of the colloidal AuNP, thereafter attachment of the peptides on the AuNP surface self-assembly. There are studies in the literature by means of their easy fabrication method. It was shown that aggregation, stability, and growth of the NPs are controllable by peptide modification of AuNPs in aqueous solution [112]. In another study, it was demostrated that, the position of the N-terminal and the aromatic groups in the sequence are significantly effective on the assembling of the nanoparticles [113].

For modification of AuNPs with peptides, the peptides can be added into AuNPs suspension in an aqueous media, and the adsorption occurs naturally through ionic, hydrophobic, and Van der Waals interactions. There are three criteria for the peptide-AuNP bioconjugation: 1) pH value during the binding reaction, 2) pI value of the peptide, and 3) quantity of the peptide. There are different approaches about relationship between the pI value and the pH value in the bioconjugation. The general statement is that the peptides/proteins bind most effectively to the AuNP surface at the pH near their pI value [114]. In another study, it was found that higher pH then the pI cause to decrease adsorption of IgG on GNPs. On the other hand, it was obtained that basic pH values were convenient for the immunoglobulins with high pI [115]. The quantity of the peptide to be

bonded onto AuNP surface is another unclarified issue. Although it was reported as the higher protein excess the higher specific activity [116, 117], the addition of them to the reaction media may cause to detachment of protein from the AuNP surface [118]. Thus, the parameters must be optimized as for each bioconjugation reaction [86].

1.3. PROSTATE CANCER

Prostate cancer is a type of cancer occurs in prostate gland, which is placed in male reproductive system (Figure 1.5). Along with slow growth of the prostate tumor, there are also fast growing types. Protate cancer can separate to the other tissues particularly bone and lymph. Its symptomes occurs as difficult urinating, blood in urine, pain in pelvis and/or dorsa at early stages. Then protration is occurred at the advance stages causing by decreasing of red blood cells.

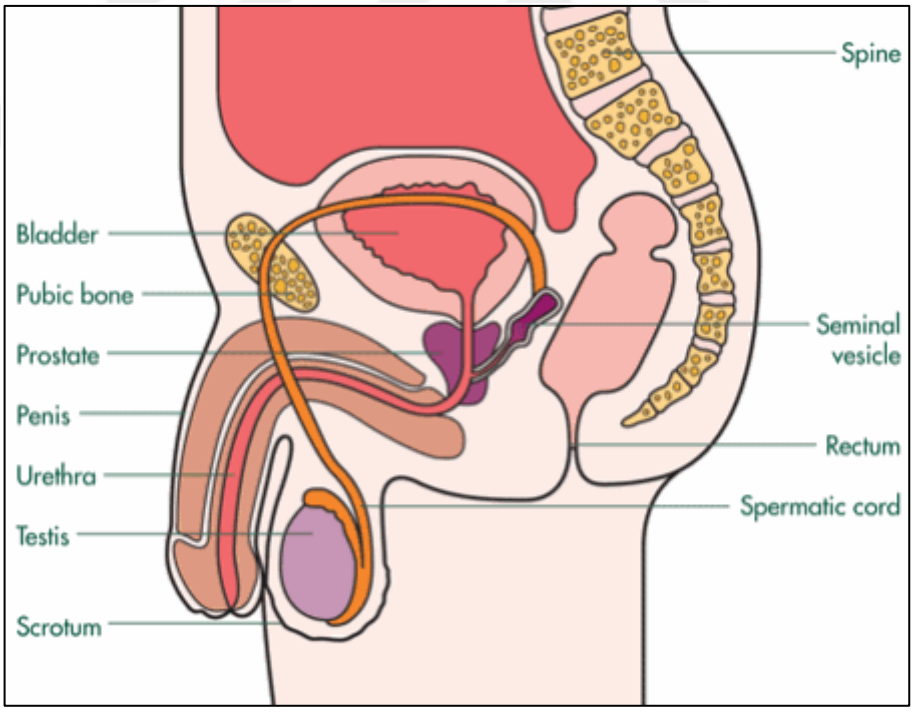

Figure 1.5. The prostate diagram [119].

Prostate cancer is the second most common cancer type in the world and the 5th cancer-related death reason among men [110]. Although its cause is not exactly determined, factors that cause the risk can be count as age, family history of disease, and ethnic background. It is mostly obtain over 50 years old, and in developed countries.

Additionally, geography has been found as another factor. Prostate cancer is most commonly seen among black men, and less common among asian men according to the American Cancer Society. Another significant factor is the diet. A diet high in red meat and dairy product, and poor in certain vegetables may be cause to cancer [121–123].

1.3.1. Diagnosis and Therapy Approaches for Prostate Cancer

The diagnosis of prostate cancer is traditionally obtained by biopsy. Then, medical imaging may be performed to determine whether the cancer has spread to other tissues in the body. Although prostate specific antigen test is efficient for diagnosis, it has not any curing effect on the desease. Thus, its application is controversial [124].

Treatment ways of prostate cancer including surgical intervention, radiotherapy, hormone therapy, and chemotherapy [125]. Chemotherapy is not enough to treat prostate cancer, because the tumor including different type of cells and their response to chemotherapy are different from each other [126]. Also the surgery for the removing of the cancer tissue is difficult due to the location of the organ, and needed to additional techniques such as radiotherapy [127]. These methods are mostly while removing the tumor, cause damage on the healthy tissue. Chemotherapeutic drugs are also have an important place. Among them, taxane group drugs are the most efficient for prostate cancer [127]. On the other hand, the achievement of the treatment method is related with age and how aggressive the tumor is.

1.3.2. Nanotechnology in Diagnosis and Therapy of Prostate Cancer

Use of nanotechnology in therapy, diagnosis, and bioimaging is named as “nanomedicine” by the National Institutes of Health. This term is including targeting of the specific molecules by biocompatible nano-carriers, and investigating their response to therapy by less side-effects. Here is the target mostly tumor cells [32]. Upon the biopsy and its disadvantages [129], new methods have been developed for early detection and treatment. Herein, the researchers focused on mostly detection of prostate specific antigens (PSA). PSA is enzyme produced by the prostate gland cells. They are placed in blood as bound to proteins and in low concentration. The measurement of the free PSA in blood may provide an insight whether the prostate cancer or not [130]. At this point, the use NPs as

nanocarrier have great potential for both diagnosis and therapy of prostate cancer by targeting PSA [131]. On the other hand, NPs they can be used to deliver active substance to the tumor [132]. It was demonstrated that epigallocatechin-3-gallate (EGCG) [133], which causes to apoptosis in prostate cancer cells, coated NPs bind to PSA selectively [134]. In addition, it was found that curcumin also has anticancer effect on prostate cancer cells [135]. Upon this, curcumin was given to the cancerous cells with PLGA NPs. Consequently, the curcumin loaded PLGA NPs showed enhanced activity on the cancer cells comparing with naked curcumin [136].

The another cyctotoxic molecule for prostate cancer cells boswellic acid [137] was prepared as NP, and it was investigated that these NPs showed apoptotic effect on prostate tumor (PC3) without causing any damage in healthy tissue [138]. On the other hand, PSMA (prostate-specific membrane antigen) is another biomarker for diagnosis of prostate cancer. Upon this, in a study peptide based nano platform was designed, and indicated their capability for selectively binding to PSMA [139]. It was also reported that, PSMA modified GNPs RNA aptamer has potential use in both targeting and therapy of prostate cancer [140]. Additionally, there are studies in the litrature about that, the peptides have potential use to enhance cellular uptake [141, 142].

2. AIM OF THE STUDY

AuNPs have a great potential to be used in many medical applications such as drug delivery, specific biomolecule targeting, and therapy due to their unique optical properties, biocompatibility, stability and tunable surface chemistry. In this study, it was aimed that providing efficient bioconjugation between the AuNPs and the various peptides, and evaluating the cellular response to altered AuNP surface for both PNT1A (Normal prostate epithelium immortalized with SV40) and DU145 (prostate cancer cells expressing the recombinant androgen receptor) cell lines.

3. MATERIALS

3.1. CHEMICALS AND KITS

3.1.1. AuNPs

Gold (III) chloride trihydrate ($HAuCl_4 \cdot 3H_2O$, M_W:393.83 g/mol) (Sigma-Aldrich #520918, USA), trisodium citrate dihydrate ($C_6H_5Na_3O_7 \cdot 2H_2O$, M_W:294.10 g/mol) (Merck #A829748, Germany).

3.1.2. Peptides

The peptides were purchased by considering their sequence, length and charge (Table 3.1). All the peptides were purchased as lyophilized powder and 10±0.2 mg. The each samples were dissolved in 1.0 ml ddH_2O (18.2 M.Ω.cm) and stored at -20ºC. Molecular structures of the peptides were as given in Figure 3.1.

Table 3.1. The sequences, molecular weights, isoelectric points and charges of the peptides used to modify the surfaces of 13 nm AuNPs.

Code	Sequence	M_w (g/mol)	pI	Net charge at pH 7
Pep1	H-Glu-Glu-Glu-Cys-OH	508.50	3.67	(-)3.1
Pep2	H-Cys-Glu-Glu-Glu-OH	508.50	3.67	(-)3.1
Pep3	H-His-His-His-Cys-OH	532.58	7.32	(+)0.2
Pep4	H-Cys-His-His-His-OH	532.58	7.35	(+)0.2
Pep5	H-Asp-Gly-Arg-Glu-Glu-Glu-Cys-OH	836.83	3.54	(-)3.1
Pep6	H-Cys-Glu-Glu-Glu-Arg-Gly-Asp-OH	836.83	3.54	(-)3.1

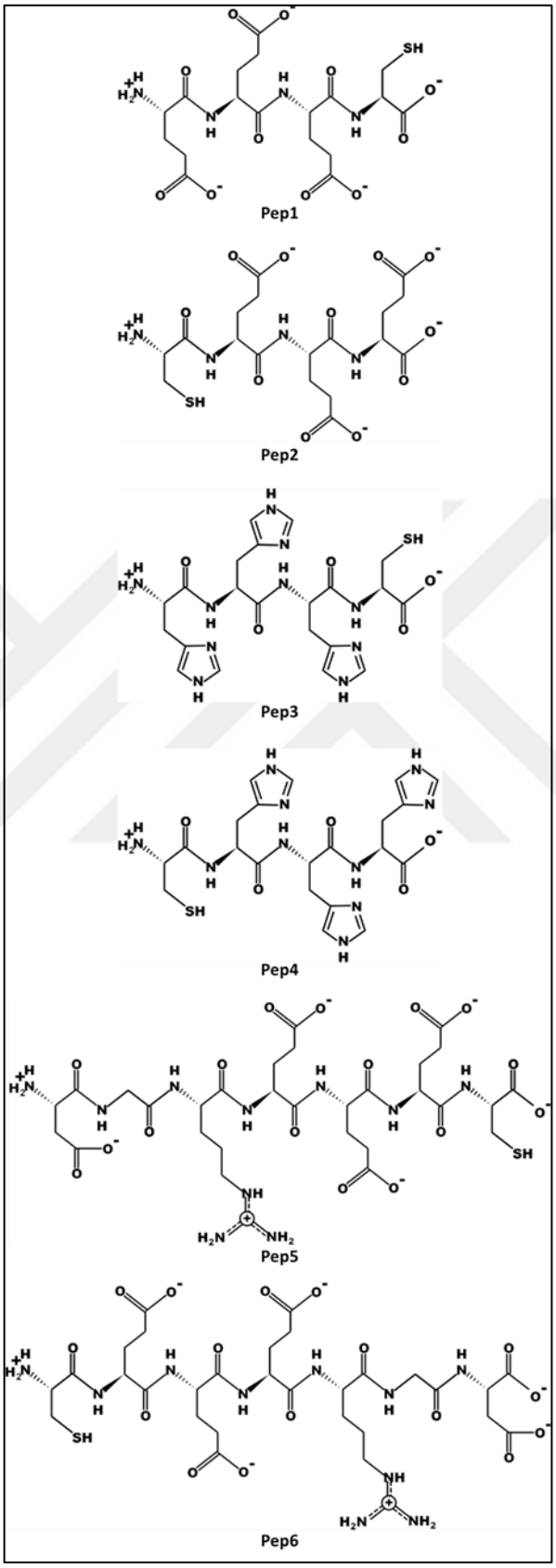

Figure 3.1. Molecular structures of the peptides.

3.1.3. Cell Culture Reagents and Kits

Dulbecco's Modified Eagle's Medium - High Glucose (Gibco #41966029, UK), Fetal Bovine Serum (FBS) (Gibco #10270, UK), phosphate buffered saline (PBS) (HyClone™, USA) (Gibco #SH30256, USA), Penicillin Streptomycin (10,000 U/ml) (Gibco #15140122, USA), Trypsin-EDTA 0.25 per cent (Sigma-Aldrich #T4049, USA), Cell Proliferation Reagent WST-1 (Roche #05015944001, USA), Dead Cell Apoptosis Kit with Annexin V FTIC and PI (Invitrogen #BMS500FI, Austria) were used for cell culture studies. Tissue culture flasks (25 cm^2, 75 cm^2), 24 and 96 well plates, Falcon tubes (15 ml and 50 ml), serological pipettes (TPP, Switzerland).

3.2. CELL LINES

Normal human prostate cell line (PNT1A, #95012614, Sigma-Aldrich, Germany) and human prostatic carcinoma cell line (DU145, HTB-81, ATCC, USA) were used as model cell lines in this study.

3.3. INSTRUMENTS

UV/Vis spectrometer (PerkinElmer, USA), Zetasizer Nano-ZS (Malvern Insturements, UK), FT-IR spectrometer (Thermo NICOLET IS50, USA), TEM (JEOL-2100 HRTEM LaB_6 JEOL, USA), benchtop pH/mV meter (Hanna Instruments HI 2211, USA), mini-shaker (Multi Bio 3D Biosan, Latvia), 2-5 centrifuge (Sigma, UK), Gel Electrophoresis System (Bio-Rad, Germany), mikro 22R centrifuge (Hettich, UK), Biohazard safety cabinet (Esco Class II type A2, USA), CO_2 incubator (37^oC, CO_2 5 per cent, Nuaire, USA), ELx800 Absorbance Reader (Biotek, USA), Flow Cytometer (Guava easy-Cyte5, Merck Millipore, Germany) were used in this study.

4. METHODS

4.1. SYNTHESIS OF GOLD NANOPARTICLES

Synthesis procedure of 13 nm gold nanoparticles were performed by the classical citrate reduction method [44, 143]. Before the synthesis all the glassware were treated with aqua regia to remove any noble metals. 80 mg tetra chloro auric acid ($HAuCl_4.3H_2O$) in 200 ml ddH_2O was heated and stirred until boiling. Then, 10 mL of 38.8 mM sodium citrate dihydrate ($C_6H_5O_7Na_3.2H_2O$) solution was added into the boiled solution quickly. Boiling was continued for 15 minutes. The final AuNP suspension was left to cool at room temperature. It was stored at room temperature and in dark until characterization.

4.2. MODIFICATION OF GOLD NANOPARTICLES WITH THE PEPTIDES

The gold nanoparticles were modified with the peptides differing in sequence, length, and charge. The pH of the AuNP suspension was adjusted by using 0.1 and 0.5 M NaOH, and 0.1 M HCl. 20 µl of 1.0 mg/ml peptide solutions were added to 1.0 ml of 13 nM AuNP suspension at proper pH and room temperature in 1.5 ml Eppendorf centrifuge tubes. The amount of peptides attached on AuNPs and proper pH values were optimized. The peptide-AuNP mixes and 13 nm AuNP suspension were mixed by the mini-shaker overnight. Since the all peptides were designed as included cysteine amino acid, they did not need any spacer molecule for binding to AuNPs surfaces. Peptide functionalized AuNPs were washed with ddH_2O (18.2 M.Ω.cm).

4.3. CHARACTERIZATION OF THE GOLD NANOPARTICLES AND GOLD NANOPARTICLES WITH THE PEPTIDES

The bare AuNPs and the AuNP-Peptide conjugates were characterized by UV/Vis spectroscopy, DLS, 1 per cent agarose gel electrophoresis, and FTIR.

4.3.1. UV/Vis Spectroscopy

The absorbance spectra of 13 nm AuNPs, and AuNP-Peptides were observed by scanning the wavelength range of 200-800 nm with UV/Vis spectrometer.

The AuNP and the AuNP-Peptide suspensions were diluted 1:10 in ddH_2O to be characterized by UV/Vis spectroscopy.

4.3.2. Dynamic Light Scattering

Hydrodynamic size of the synthesized 13 nm AuNPs and the AuNP-Peptide conjugates were measured by DLS. The measurements were carried out as repeated three times at room temperature, 173° scattering angle, and 4 mW He-Ne laser was used as the light source. The 1:10 diluted colloidal solutions were placed into polystyrene cuvettes for the measurements, and for the surface charge measurements, disposable capillary cells were used.

4.3.3. Transmission Electron Microscopy Analysis

13 nm AuNPs were characterized by Transmission Electron Microscopy (TEM). For the measurements, drops from the colloidal gold samples placed onto carbon supported copper TEM grids.

4.3.4. Fourier Transmission Infrared (FTIR) Spectroscopy Analysis

The naked AuNPs and the AuNP-Peptides were characterized by FT-IR between the wavelength range of 4000 cm^{-1}-400 cm^{-1}. For the sample preparation, the colloidal solutions were centrifuged at 13000 rpm for 30 min and the precipitates were washed with ddH_2O. The water-dispersed samples were stored at -80^{0}C overnight, and dehydrated by freeze-dryer.

4.3.5. Agarose Gel Electrophoresis

The AuNPs and the conjugates were analyzed by 1 per cent agarose gel electrophoresis (AGE) to determine the peptide bonding on the AuNPs surfaces. The colloidal solutions were centrifuged at 13000 rpm for 30 min. The precipitates were washed with ddH_2O, and re-dispersed in 20 µl ddH_2O. The gel tank was placed onto ice to keep the environment ice-cold. The samples were loaded into the wells of the gel prepared by 1x TAE buffer, and electrophoresed at 100 V for an hour. No staining procedure was required due to the advantage of the AuNPs samples being colored. After completion of the electrophoresis, the gel was photographed.

4.4. CELL CULTURE

PNT1A human normal prostatic and DU145 prostate cancer cell lines were both treated with the developed nanomaterials for comperatively observation of the cellular response. 10 per cent FBS and 1 per cent PS containing high glucose DMEM was convenient media for the both cell lines. For cell growth, 37°C and 5 per cent CO_2 humidified atmosphere was provided by a cell culture incubator.

4.5. TREATMENT OF THE CELLS WITH THE PEPTIDE FUNCTIONALIZED GOLD NANOPARTICLES

PNT1A and DU145 cells were seeded as 40000 cells/well in 24-well plates and incubated for 24 h. After the attachment provided, the cells were treated with increasing final concentation (0.1, 0.5, 1.0, and 2.5 nM) of the AuNPs and the AuNP-Peptides for 24 h.

4.6. APOPTOSIS/NECROSIS ASSAY

To evaluate the cell death mechanism, Annexin-V and PI staining were performed. First, cell detachment was iniciated by 0.25 per cent Trypsin-EDTA solution. Then, cell culture media was added as twice amount of trypsin into the each well to stop the trypsin activity. The cells were collected in eppendorf test tubes, and harvested by centrifugation at 2500

rpm for five min. After PBS washing, the pellets were resuspended in 200 µl of 0.5 µl Annexin-V containing 1x binding buffer. The samples were kept in the dark for 10 min. After centrifugation, the cells were dispersed in 1.0 µl PI containing 200 µl 1x binding buffer. Following the staining procedure, the samples were analyzed by flow cytometry as soon as possible.

4.7. WST-1 CELL PROLIFERATION ASSAY

For WST-1 assay, 6000 cells were seeded on each well of 96-well plates. After the NPs treatment for 24 h, the supernatants were removed, and the cells were washed with PBS. Thereafter, the cells were incubated with 5 per cent WST-1 reagent containing complete medium for 1 h at 37°C, and 5 per cent CO_2 in a humidified incubator. Following the incubation, the supernatants were transferred to the new 96-well plates. When the tetrazolium salts were converted into formazan crystals, which can be investigated by colorimetry, the absorbance values of the samples were measured by a microplate reader at 450 nm of wavelength.

4.8. CELL CYCLE ANALYSIS

For cell cycle assay, the both cell lines were seeded as 40000 per well on 24-well plates. After the period for cell attachment, the cells were treated with 0.1, 0.5, 1.0, and 2.5 nM of the AuNP-Peptides for 24 h. Following the treatment, cell dissociation was provided by incubating with Trypsin-EDTA at 37ºC, 5 per cent CO_2 for 5 min. Thereafter the initiate the trypsin effect, the suspensions were transferred to the 1.5 ml Eppendorf test tubes, and centrifuged at 2500 rpm, 4ºC for 5 min. Subsequently, the supernatant was decanted, and the harvested cells resuspended in 70 per cent ethanol solution for fixation. The fixed cells were kept at -20ºC for at least 2 h to be prepared for labeling. After the centrifugation at the same conditions, the cells were resuspended in 0.1 per cent 500 µl Triton X-100 prepared in 1x PBS, and kept at room temperature for 20 min. Thereafter, the cell suspensions were centrifuged, and resuspended in 200 µl of 0.3 mg/ml RNAse prepared in 1x PBS. The suspensions were kept at 37ºC for 30 min in an incubator. After the incubation, the cells were resuspended in 200 µl of 5 mg/ml PI prepared in 1x PBS. The

suspensions were kept at 4ºC in dark for at least 15 min. Then, the PI stained cells were analyzed by flow cytometry.

5. RESULTS AND DISCUSSION

5.1. CHARACTERIZATION OF THE GOLD NANOPARTICLES AND THE GOLD NANOPARTICLES WITH THE PEPTIDES

Characterization of the synthesized AuNPs, and AuNP-Peptides were performed using UV/Vis spectroscopy, Dynamic Light Scattering (DLS), FT-IR, Agarose Gel Electrophoresis.

5.1.1. AuNPs

The synthesized AuNPs were characterized by UV/Vis spectroscopy, DLS, and TEM taking advantage of their unique light absorption properties due to their plasmonic features. There is a relationship between the maximum absorbance of the AuNPs and their size according to the dipol-dipol interaction among the AuNPs [144, 145]. In addition, the color change from red to purple is occurred in relation to the size and/or agglomeration [146, 147]. The white light image of the synthesized wine red 13 nm AuNP suspension is presented in Figure 5.1. On the UV/Vis absorption spectrum, the λ_{max} found as 519 as can be seen in Figure 5.2 (A).

Figure 5.1. White light image of the 13 nm AuNPs colloidal suspension.

The DLS spectrum is shown in Figure 5.2 (B), which gives the hydrodynamic sizes of the AuNPs. The TEM image also provide the size of the bare AuNPs which can be seen in Figure 5.3. As seen, the average size of AuNPs is 13 nm.

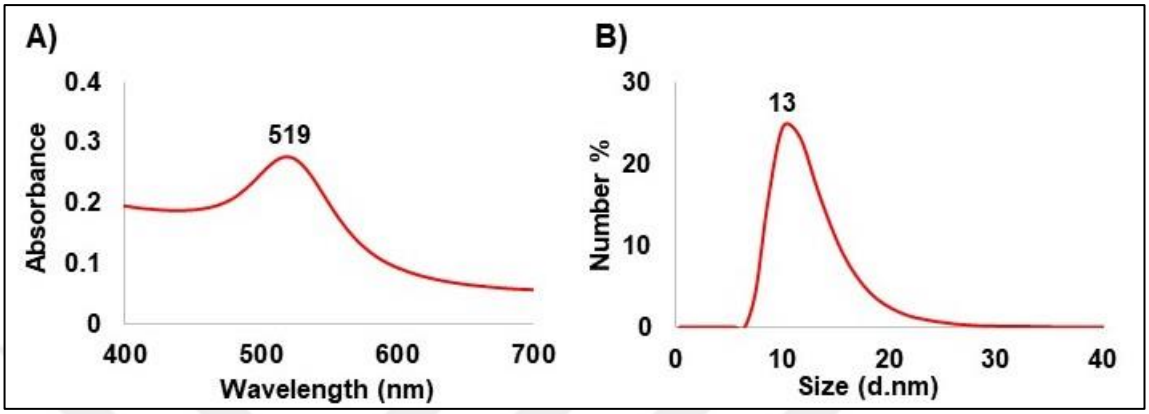

Figure 5.2. A) UV/Vis B) DLS spectrum of the synthesized AuNPs.

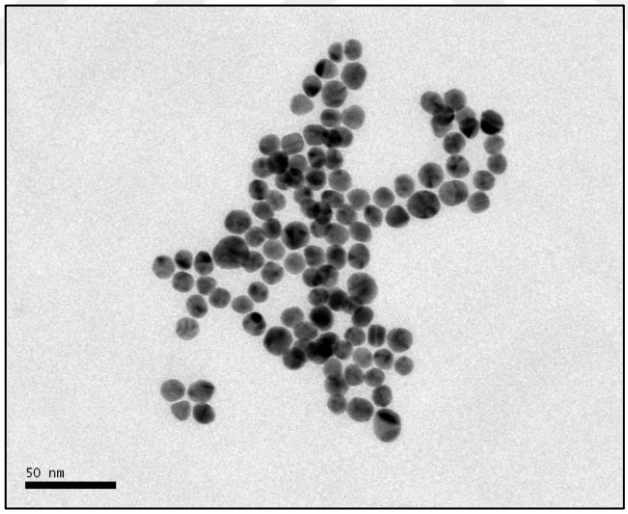

Figure 5.3. TEM image of colloidal AuNPs.

5.1.2. Peptide Modified AuNPs

The surfaces of the 13 nm AuNPs were modified with the six peptides that differ in length, sequence, and charge. They can be seen in Table 5.1 with their sequences, isoelectric points, and charges. The four peptides were four amino acids long, and the other two were

consisted of seven amino acids including RGD sequence. Since the RGD motif is known to enhance intracellular uptake of NPs [148], the peptides were designed with or without RGD motif at the end of their sequences. Thus, in the presence or absence of RGD on AuNPs surfaces can affect the degree of nanoparticle association with the cellular membrane influencing the response of the cell. Another parameter that was investigated is the difference in their charge. Amino acids, histidine (H), glutamic acid (E) and glycine (G) are used to modify the overall peptide charge. Since the charge of the RGD squence is zero, the presence or absence of RGD motif in the peptide sequence did not affect the net charge of the peptides. All the peptides were designed to have cysteine (C) at the end of their sequence due to the high affinity of the thiol group to bind to AuNP surface. In addition, the peptides are occurred with three different amino acid sequences, so they can be assumed as three peptide pairs. They have two residues $-NH_2$ and -COOH resulting from the amino acid structure. One peptide sequence starts from the $-NH_2$ end, and the other starts from the -COOH end, i.e. the amino acid sequence is inverted from the $-NH_2$ end to the -COOH end. This allowed the investigation of the influence of free $-NH_2$ or -COOH ends on the cell behavior.

Table 5.1. The sequences, isoelectric points, and charges of the peptides used to modify the surfaces of 13 nm AuNPs.

Code	**Sequence**	**pI**	**Net charge at pH 7**
Pep1	H-Glu-Glu-Glu-Cys-OH	3.67	(-)3.1
Pep2	H-Cys-Glu-Glu-Glu-OH	3.67	(-)3.1
Pep3	H-His-His-His-Cys-OH	7.32	(+)0.2
Pep4	H-Cys-His-His-His-OH	7.35	(+)0.2
Pep5	H-Asp-Gly-Arg-Glu-Glu-Glu-Cys-OH	3.54	(-)3.1
Pep6	H-Cys-Glu-Glu-Glu-Arg-Gly-Asp-OH	3.54	(-)3.1

5.1.2.1. Behaviour of the AuNP-Peptide Conjugates in Aqueous Media

In light of the literature, optimum concentration of the peptides coated on the AuNP surfaces was determined as 1 mg/ml [149]. pH values needed for the conjugation were also optimized in consideration of the isoelectric points. In many studies, only isoelectric points (pI) of peptides were considered for functionalization of AuNPs with peptides . The pH of the AuNP suspension was adjusted close to the pI of the peptide. In this case, it is said that the electrostatic repulsion between the peptide and the NP is reduced, and the peptides are immobilized irreversibly on the AuNP surface [114]. Based on this approach, the pH of the synthesized and filtered AuNP suspension was measured and found as 5.8 at room temperature. pI values of Pep1 and Pep2 were calculated to as 0.88 and 0.76. Thereafter, the pH of AuNPs suspension was adjusted to 3.0, which is closer to the pI values of these two peptides. Then, 20 µl of 1 mg/ml Pep1 solution was added to 1 ml of AuNP suspension in an Eppendorf test tube, and it was observed that the color of the suspension returned from the red to the blue. On the contrary, when 20 µl of 1 mg/ml Pep2 was added to 1 ml of AuNP suspension, no color change was observed. The blue color indicates agglomeration of the NPs unlike the red color. The visual result at the inconvenient pH condition can be seen comparatively in Figure 5.4.

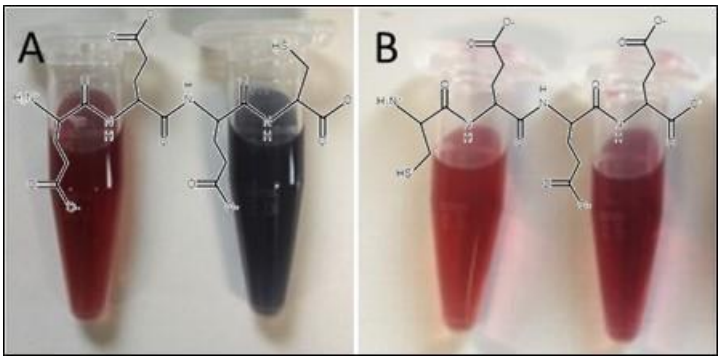

Figure 5.4. Images of the AuNP suspensions before and after peptide addition.
(a) Pep1 (b) Pep2

Although the pH of the AuNP suspension was close to pI values of Pep1 and Pep2, their conjugation results were obtained as different from each other. As well as behavior of the peptides is directly related to pH, it is shown that peptides with the same sequence and pI value may bind to AuNP surface at different pH values. However, the surface of the

AuNPs could be modified with Pep2, which has cysteine at the N-terminal, it could not be modified with Pep1, which has cysteine at its C-terminal. This finding indicates that position of cysteine amino acid in the peptide sequence is as crucial as pI value for binding of peptides to AuNP surface. Therefore, the pH adjustment was carried out by adding 0.1 M HCl or 0.1 and 0.5 M NaOH into AuNPs suspension for all the peptides. Before the conjugation, it was indicated that the colloidal AuNPs is stable in the pH range of 3.0-12.0 as seen in Figure 5.5.

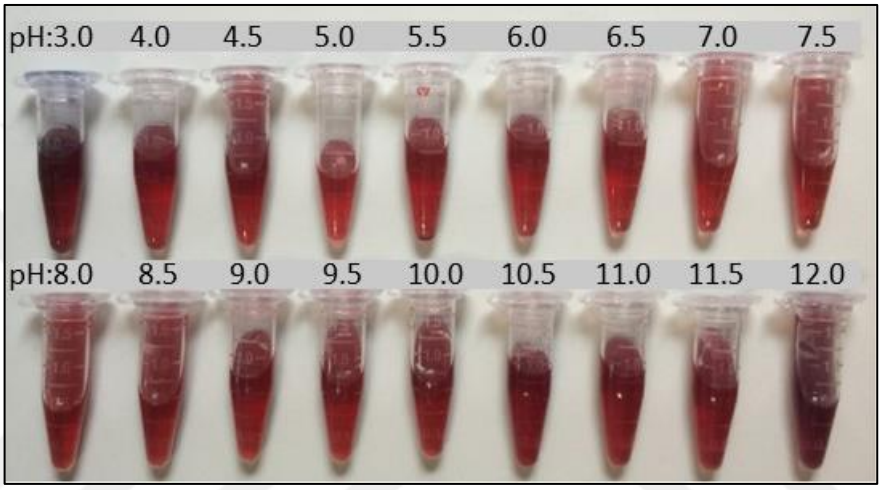

Figure 5.5. The AuNPs suspensions at various pH in range of 3-12.

After determination of stability of the AuNPs in the pH range of 3.0-12.0, 20 µl of 1 mg/ml peptide solutions were added to the AuNP suspensions at various pH values in this range, and the behavior of the AuNPs in the suspensions was observed. After the optimization process, needed pH ranges for the conjugation of all the peptides with AuNPs were determined, and recorded as in Table 5.2. Thereafter, modification of the AuNPs with the all peptides were performed. Before the functionalization, pH of the AuNPs suspension was adjusted in consideration of the determined pH ranges.

Table 5.2. The peptides sequences and the needed pH conditions for the stable AuNP-Peptides in aqueous media.

Code	Sequence	pH
Pep1	H-Glu-Glu-Glu-Cys-OH	5.5-12.0
Pep2	H-Cys-Glu-Glu-Glu-OH	3.0-12.0
Pep3	H-His-His-His-Cys-OH	10.5-12.0
Pep4	H-Cys-His-His-His-OH	10.0-12.0
Pep5	H-Asp-Gly-Arg-Glu-Glu-Glu-Cys-OH	5.5-12.0
Pep6	H-Cys-Glu-Glu-Glu-Arg-Gly-Asp-OH	4.5-12.0

Then, the AuNP-Peptides were characterized by UV/Vis spectroscopy, DLS, FT-IR, and AGE. According to the results, the conjugation of AuNPs with Pep2, Pep5, and Pep6 carried out at pH 5.8, which is the pH of AuNP suspension at room temperature without any adjustment, and they were modified with Pep1 at pH 8.6, with Pep3 at pH 11.5, and with Pep4 at pH 11.0. After the functionalization, the suspensions were observed as stable as seen in Figure 5.6. Also, modification of 13 nm AuNP with the six peptides is schematically shown in Figure 5.7.

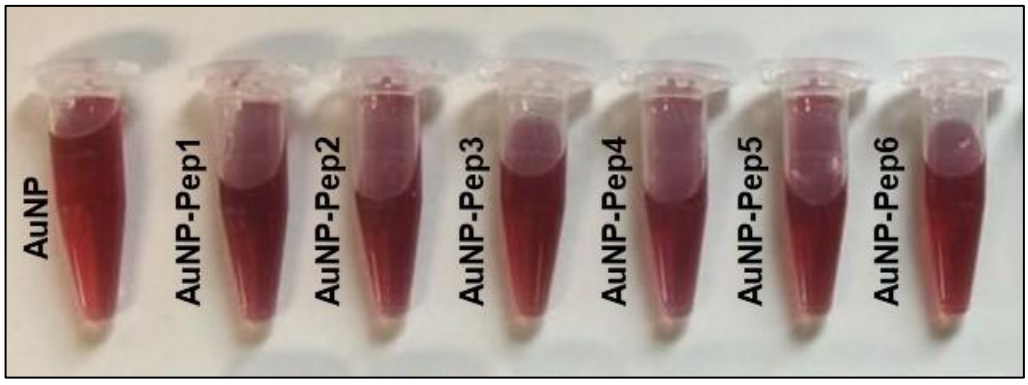

Figure 5.6. The AuNP-Peptide suspensions.

Table 5.3. Needed pH values for the AuNP-Peptide conjugation reactions.

Peptide Code	**pH**
Pep1	8.6
Pep2	5.8
Pep3	11.5
Pep4	11.0
Pep5	5.8
Pep6	5.8

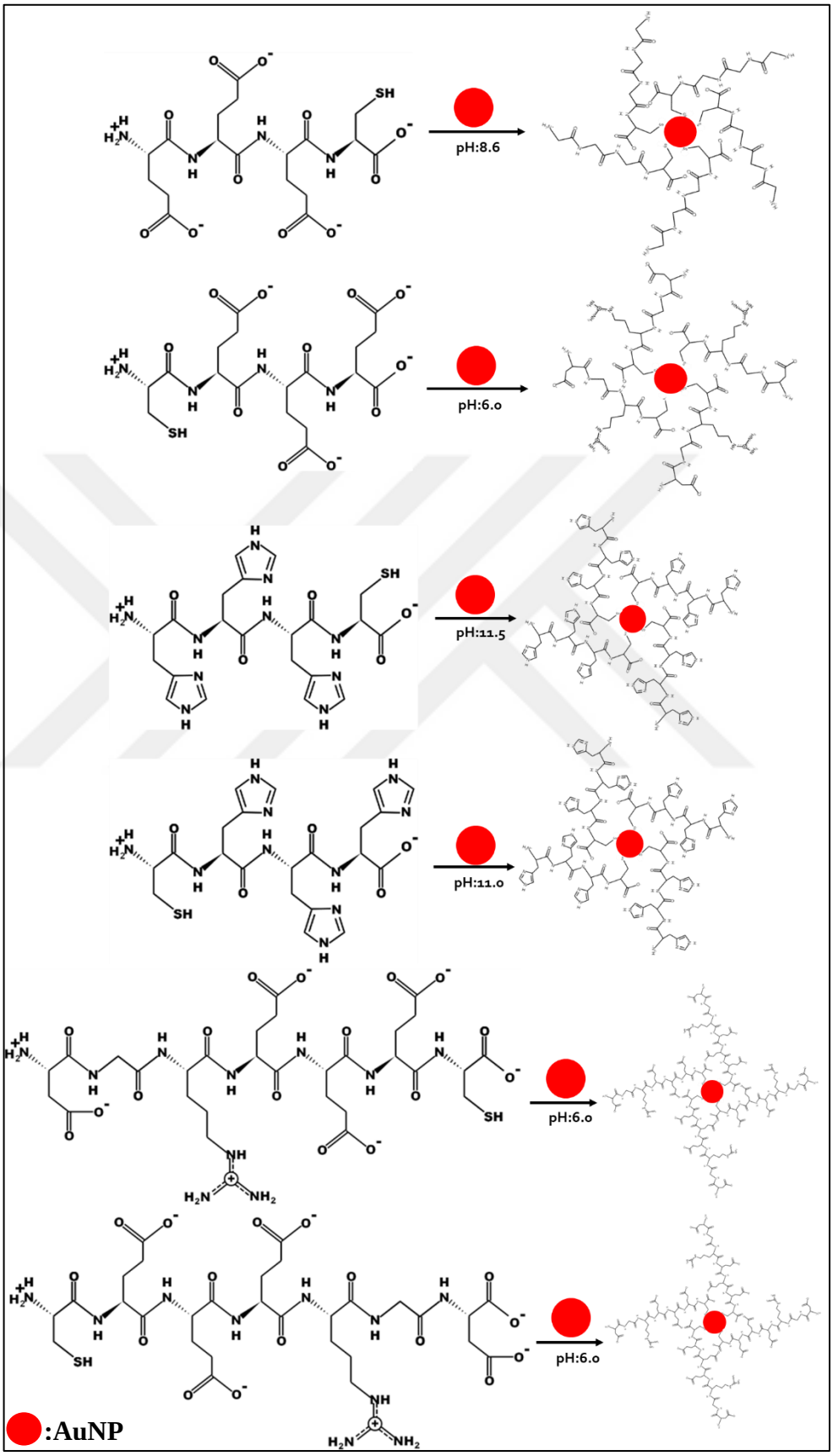

Figure 5.7. Shematical representation of the AuNP-Peptide bioconjugation reactions.

5.1.2.2. UV/Vis Spectroscopy

Bare 13 nm AuNPs and AuNPs functionalized with peptides were characterized by UV/Vis spectroscopy. For the measurements, the AuNP and AuNP-Peptide suspensions were diluted 1:10 in ddH_2O, and placed into quartz cuvette. Subsequently, the absorbance of the samples were measured by scanning between 200 and 800 nm wavelengths. UV/Vis spectra of AuNP and AuNP-Peptides can be seen comparatively in Figure 5.8. While 13 nm bare AuNPs exhibited maximum absorption at 519 nm, which is also as indicated in literature [150], the absorption peaks of peptide modified AuNPs show red shift (1-4 nm). The maximum absorption peaks of AuNPs functionalized with Pep1 were shifted 1 nm, AuNPs functionalized with Pep2, Pep3, and Pep4 shifted 2 nm, Pep5 and Pep6 functionalized AuNPs shifted 3 nm. As it is well kown that AuNPs have high affinity with thiol (R-SH) and amine (R-NH_2) groups, which are named as auxochrome groups. These groups cause to shift to longer wavelength when they bind to chromophore group consisted material (bathochromic effect). This caused by decreasing electrostatic oscillation frequency of the material since the molecular binding. The size of the binded molecule and its affinity affect on the length of the shift. Thus, the shifting of the absorption peaks to longer wavelength indicates that the peptides are attached to the AuNP surface.

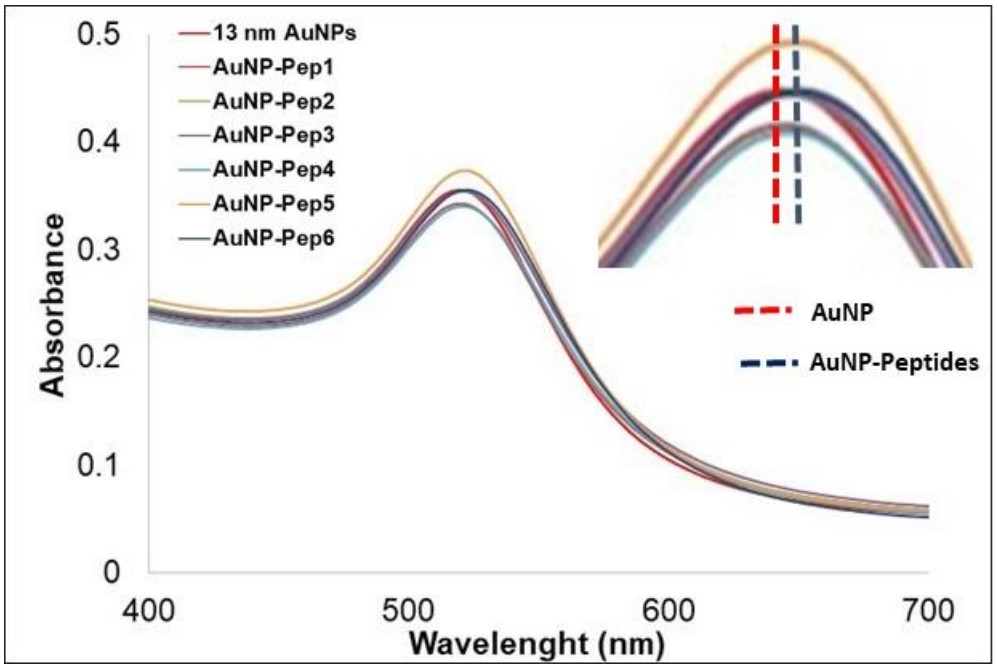

Figure 5.8. UV/Vis spectra of AuNPs and AuNP-Peptides suspensions.

5.1.2.3. Dynamic Light Scattering

Bare AuNPs and the peptide modified AuNPs were characterized by DLS to determine their hydrodynamic size and zeta potential. It is deduced diameter of the AuNPs is approximately 12 nm, and the AuNP-Peptides are larger than them according to the DLS measurements as shown in Figure 5.9.

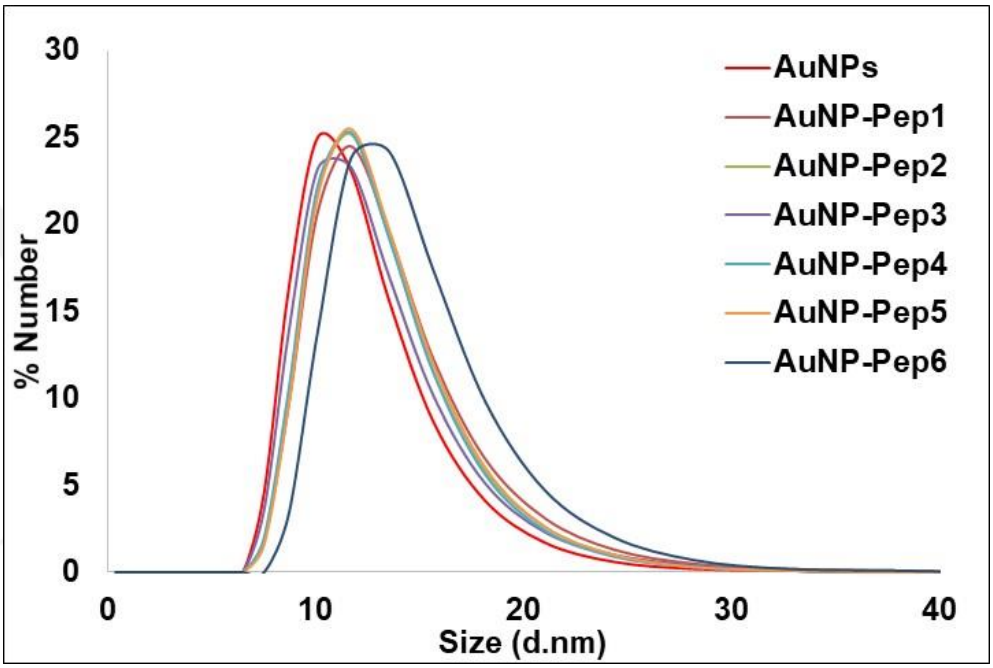

Figure 5.9. DLS spectra of AuNPs and AuNP-Peptides suspensions.

The size of the NMs, needed to be small enough to be uptaken by the cells, and large enough to be not agglomerated in liver or in any part of human body [47]. However, the larger NPs can be easier removed from the blood stream [151], the NPs are choosen as generally 20-30 nm for medical use by considering the diameter of endocytotic vesicles (40-60 nm) [47].

For Pep1, Pep3, Pep5 and Pep4 capped AuNPs, the shift is 1 nm, while 2 nm for Pep6 capped AuNPs. Additionally, zeta potential of the bare AuNPs measured as about -12 mV, and it was observed as lower for the peptide capped AuNPs. The exact size and charge values are given in Table 5.4. The changes in size and charge of the AuNPs surface indicates that the surfaces of the AuNPs are modified with the peptides.

Table 5.4. Average diameter and zeta potential values of the AuNPs and the AuNP-Peptide conjugates.

Sample	λ_{max}	Size (nm)	Zeta Potential (mV)
AuNPs	519	11.9±0.1	-11.9±0.8
AuNP-Pep1	520	12.4±0.7	-16.6±1.6
AuNP-Pep2	521	12.5±0.7	-19.9±0.3
AuNP-Pep3	521	12.2±0.2	-26.1±1.8
AuNP-Pep4	521	13.0±0.6	-30.6±0.2
AuNP-Pep5	522	12.1±0.5	-11.7±2.7
AuNP-Pep6	522	14.0±0.2	-16.5±1.6

5.1.2.4. Agarose Gel Electrophoresis

13 nm AuNPs and AuNP-Peptides were characterized by one per cent agarose gel electrophoresis to determine the peptide density on the AuNPs surface. The image of the agarose gel after run is given in Figure 5.10. Though the bare AuNPs precipitated due to the EDTA salt in the 1x TAE buffer solution, AuNP-Peptides run relating to their size and zeta potential as reported in literature [152-153]. The bands belong to the conjugates are seen clearly. This indicates that the surfaces of AuNPs in the suspension were adequately capped with the peptides. Besides, it was observed that some of the AuNP-Peptides run less than the others due to the position of cysteine (C) amino acid in the peptide suquence. When C placed at the -NH_2 end, strong bond is achieved due to the affinity of the AuNP, and relatively weak binding occurs when C placed at the -COOH end. As a result, under the specified conditions, the surfaces of AuNPs were functionalized with the peptides, and the position of the C amino acid in the peptide sequence has a significant effect on surface functionalization of AuNP with peptides.

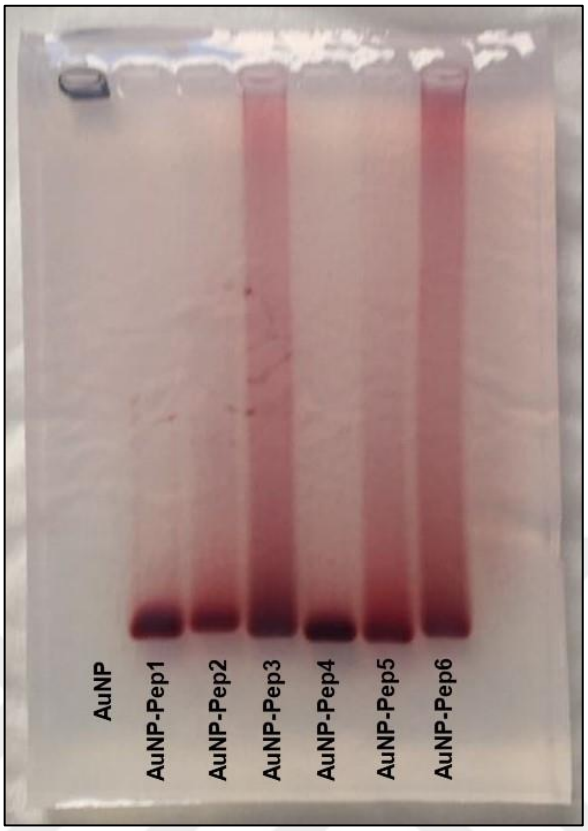

Figure 5.10. Image of 1 per cent agarose gel electrophoresis result of the peptide modified AuNPs.

5.1.2.5. Fourier Transform Infrared Spectroscopy

The bare AuNPs and AuNP-Peptides were characterized by FTIR so that molecular information can be obtained from peptides on the surface of AuNPs. FTIR spectra of the AuNPs and the peptide modified AuNPs is seen comparatively in Figure 5.11. Although, no peaks were observed in the FTIR spectra of bare AuNPs, in the AuNP-Peptide spectra, C-H stretching at 2850-2900 cm^{-1}, amide group C=O stretching at 1640-1690 cm^{-1}, amide group N-H bending at 1590-1640 cm^{-1}, 1435 cm^{-1} C-CH_3 streching, CN streching at 1080-1250 cm^{-1}, Amit I bond, C=O streching and N-H stretching bands. The bonds indicated by the spectra exist in the structures of the peptides. Thus, the modification of AuNPs with the peptide proved by the FTIR spectra.

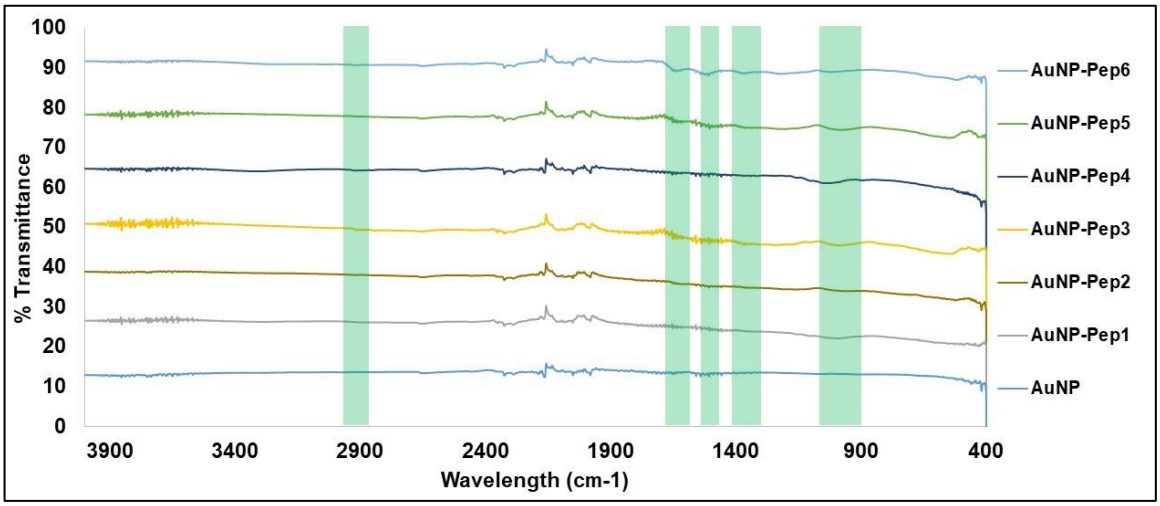

Figure 5.11. FT-IR spectra of the bare AuNPs and the AuNP-Peptide conjugates.

5.2. EFFECT OF THE AuNP-PEPTIDES ON PROSTATE CANCER CELLS

The effects of the peptide modified AuNPs on cytotoxicity and cell cycle were investigated for both normal (PNT1A) and cancer (DU145) epithelium cells comparatively. Thus, response of the cells with different metabolic characteristics to the AuNP-Peptides could be evaluated. Besides, it was shown that the AuNPs can be reproducibly modified with the biomolecules, and they are stabile in cell culture media. Also, the response of the cells to AuNPs, which were functionalized with the peptide pairs consisting the same amino acids but in reverse sequence was evaluated systematically in the presence or absence of the RGD sequence.

5.2.1. Cytotoxicity

To evaluate the cytoxicity of the AuNP-Peptides, WST-1 cell viability and Annexin-V apoptosis-necrosis assays were carried out. Concentration of the AuNP-Peptides in the media were determined as 0.1, 0.5, 1.0, and 2.5 nM in consideration of the optimization process. The both healthy and cancer cells were exposured to the AuNP-Peptides for 24 hours, and responses of the cells were examined by the indicated tests. The cells treated with 10 per cent DMSO were used as the positive control.

5.2.1.1. WST-1 Cell Proliferation Assay

WST-1 reagent consists of tetrazolium salts, and the test is based on reducing of the salts to formazan by mitochondrial dehydrogenases in living cells as represented in Figure 5.12. Since the reaction is colorimetric, it can be identified by fluorescence spectroscopy. Although WST-1 is an easy to handle cytotoxicity assay, it is error-prone relatively. Thus, another test is needed to obtain more reliable results, so apoptosis-necrosis assay was also performed in this study.

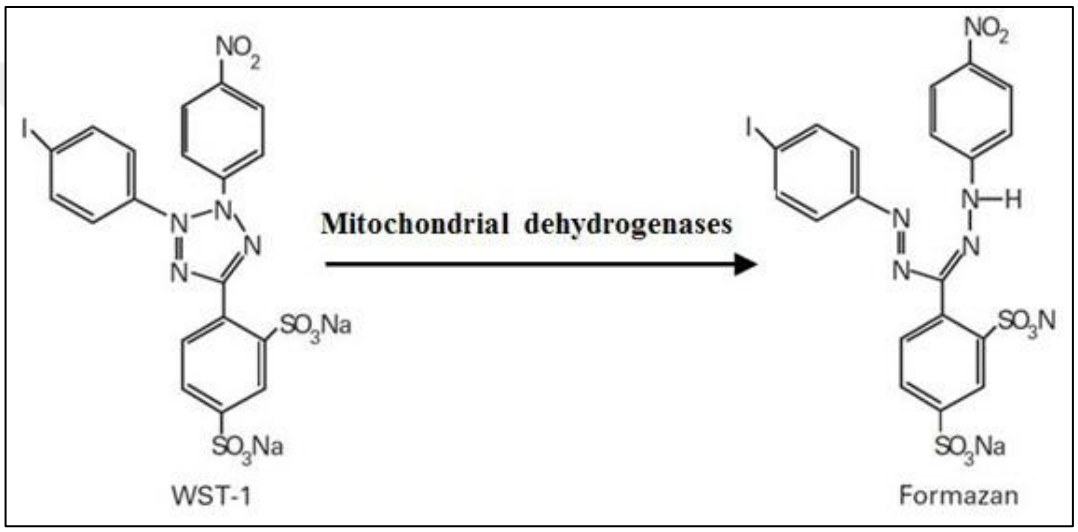

Figure 5.12. Reduction of the tetrazolium salt to formazan.

According to the WST-1 assay results, the bare AuNPs reduced the cell viability. While the bare AuNPs reduced the cell viability to around 60 per cent at 0.1, 0.5, and 1.0 nM, the viability was observed as 40 per cent for 2.5 nM AuNPs as can be seen in Figure 5.13.

As well as the greater cell viability was obtained with AuNP-Pep2, it was found as nearly the same for the other AuNP-Peptides depending on their C amino acid position. Hereupon relatively high cell proliferation was obtained for the AuNPs modified with cysteine-N-terminal peptides due to the affinity of the AuNP surface to –SH group. Here the other parameter is hydrophobicity. Thus, Pep3 and Pep4, which are the cyclic structure containing peptides showed relatively low effect on the both cell lines. Molecule size, steric hindrance, and hydrophobicity balance between the cell membrane and surface of the AuNPs cause to the difference in cellular response as well as the whether existing of RGD sequence or not. On the other hand, RGD sequence, which has significant role in the “cell

penetrating peptides" [154, 155] showed less toxicity for the cancer cell lines, and more toxicity for the healthy cell lines compared to the same sequence without RGD (Pep1 and Pep2). This may related with the molecule size and the cellular uptake.

In the light of this results, it can be deduced that peptide modification of the AuNPs reduce the cytotoxic effect on the healthy prostate cells in comparison with the bare AuNPs.

As opposed to the response of the healthy cells to the AuNP-Peptides, the cysteine-N-terminus peptide modified AuNPs show higher toxicity on the cancer cells when compared to bare AuNPs. Also AuNP-Pep1, AuNP-Pep3 and AuNP-Pep5 significantly reduced the viability of the cancer cells.

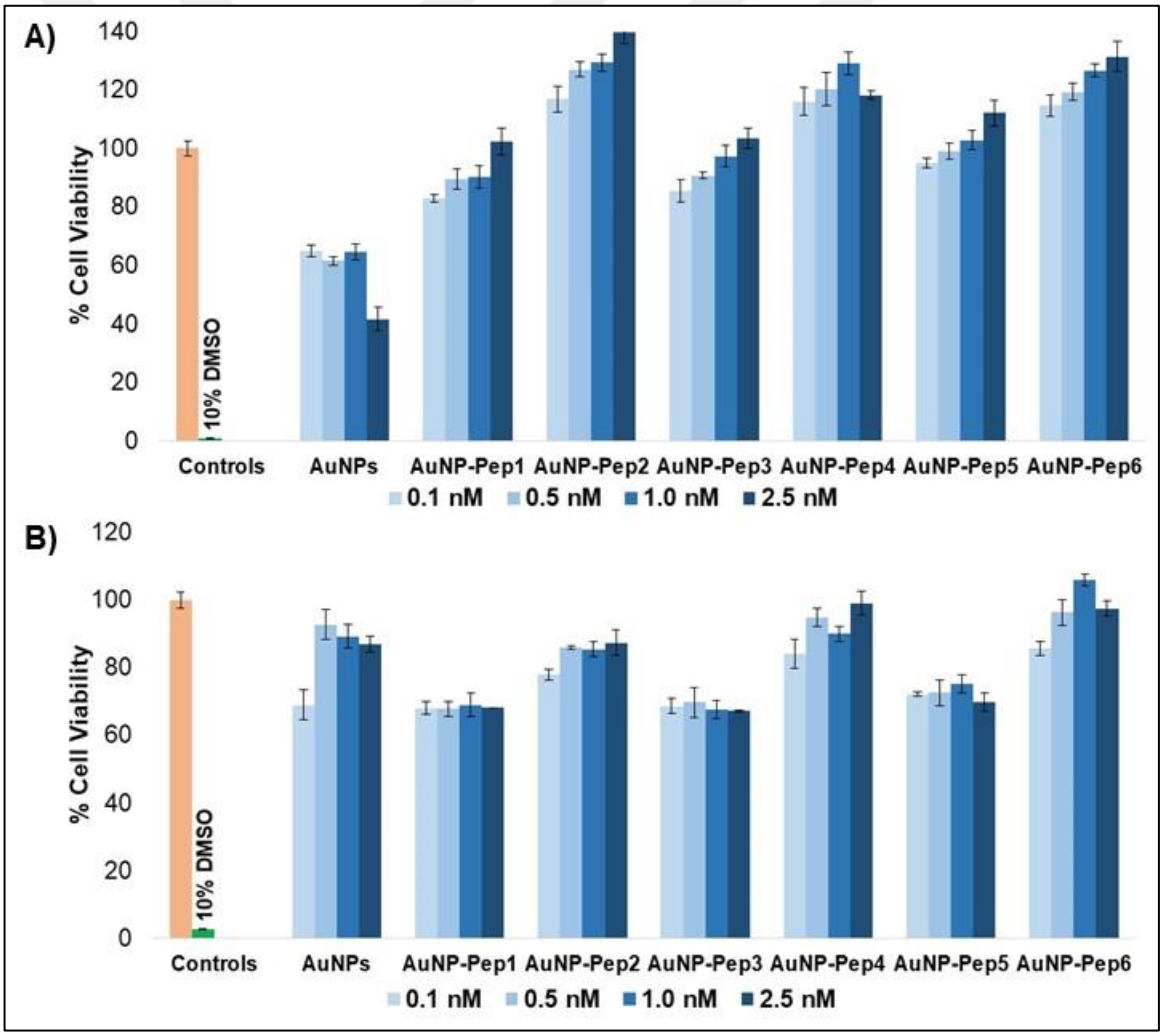

Figure 5.13. Cell viability of (a) PNT1A (b) DU145 cells at increasing concentrations of the AuNPs and the AuNP-Peptides.

5.2.1.2. Apoptosis-Necrosis Assay

Apoptosis-necrosis assay was carried out by staining the AuNP-Peptides exposured cells with Annexin V and PI dyes, and analyzing of them by flow cytometry. Annexin V binds to phosphatidylserine proteins, which are occured out of the cell membrane due to the apoptotic cell death, and PI stains to DNA. Thus, the early apoptotic cells can be observed by staining with only Annexin V, late apoptotic cells can be detected by staining with both Annexin V and PI, and necrotic cells can be detected by staining with only PI.

The toxicity of increasing concentration of the AuNPs and the AuNP-Peptides exposured cancer prostate cancer cells (DU145) was investigated by apoptosis-necrosis assay, and the results are given in Figure 5.15.

10 per cent DMSO reduced the viability of DU145 cells to about 12 per cent, and mostly caused to early apoptosis. In range of 0.1-1.0 nM concentration of the bare AuNPs led to apoptosis and necrosis of some of the cells.

The AuNP-Peptide exposured cells showed higher apoptosis ratio than the bare AuNPs exposure cells. While the most effective concentration for apoptosis was found as 2.5 nM for the four peptides, it was found as 1.0 nM for Pep3 and Pep4. 1.0 nM concentration is the optimum dosage due to the minimum toxic effect level on healthy cells as also can be seen in WST-1 results. On the other hand, effect on toxicity of location of the C amino acid in the peptide sequence shows significant difference as it also seen in the cell viability results. While the Pep1 and Pep5 modified AuNPs indicated higher apoptosis ratio, the histidine containing peptide modified AuNPs caused to obtain relatively less apoptotic cells. On the contrary of the other two peptide pairs, Pep3 and Pep4 showed difference in apoptosis ratio. Additionally, when the cysteine located at N-terminal as in Pep3 and Pep4, the high apoptosis rate is observed. AuNP-Pep4 conjugates showed higher apoptotic cell death due to the steric hindrance caused by the cyclic structure.

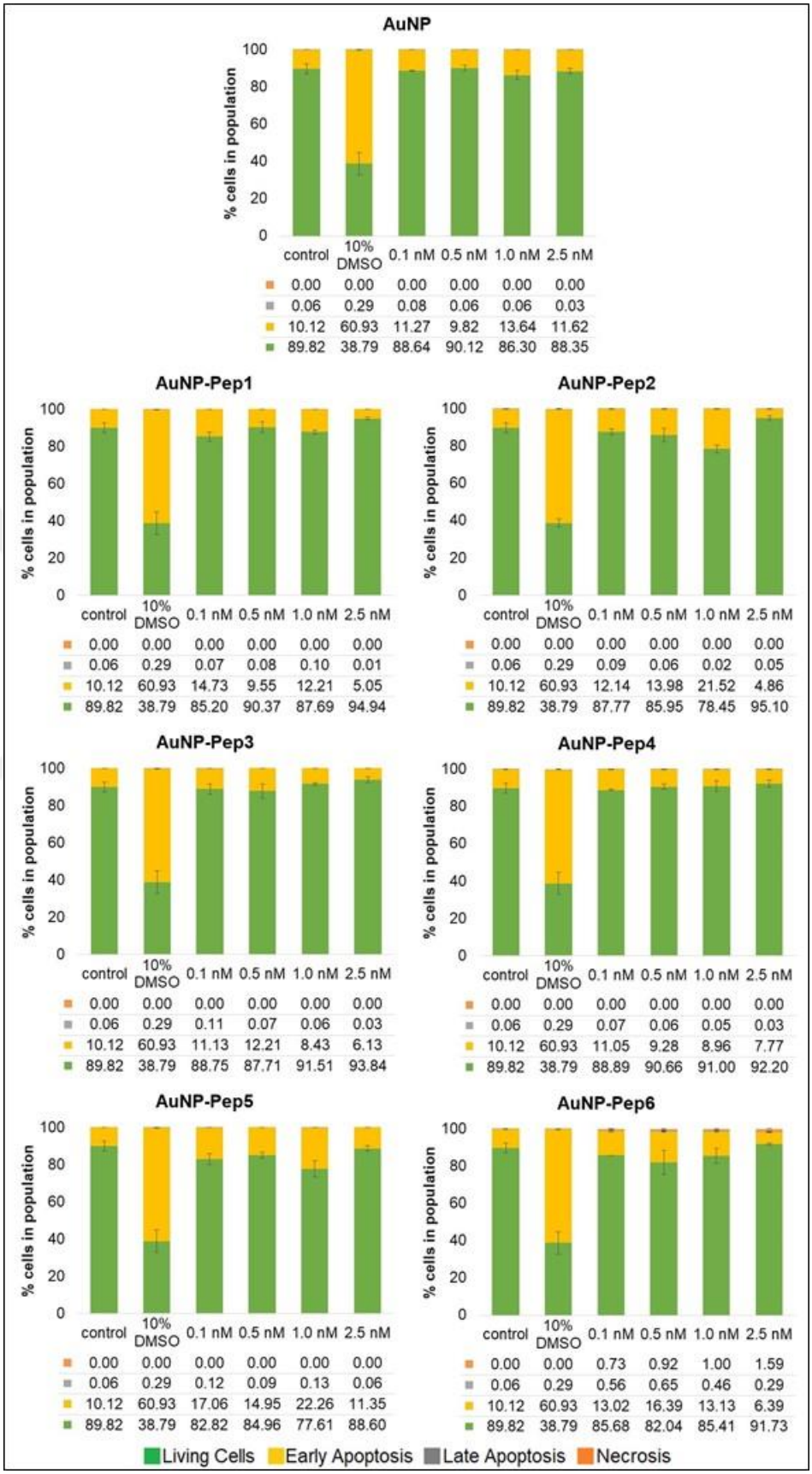

Figure 5.14. Apoptosis-necrosis analysis of PNT1A cells.

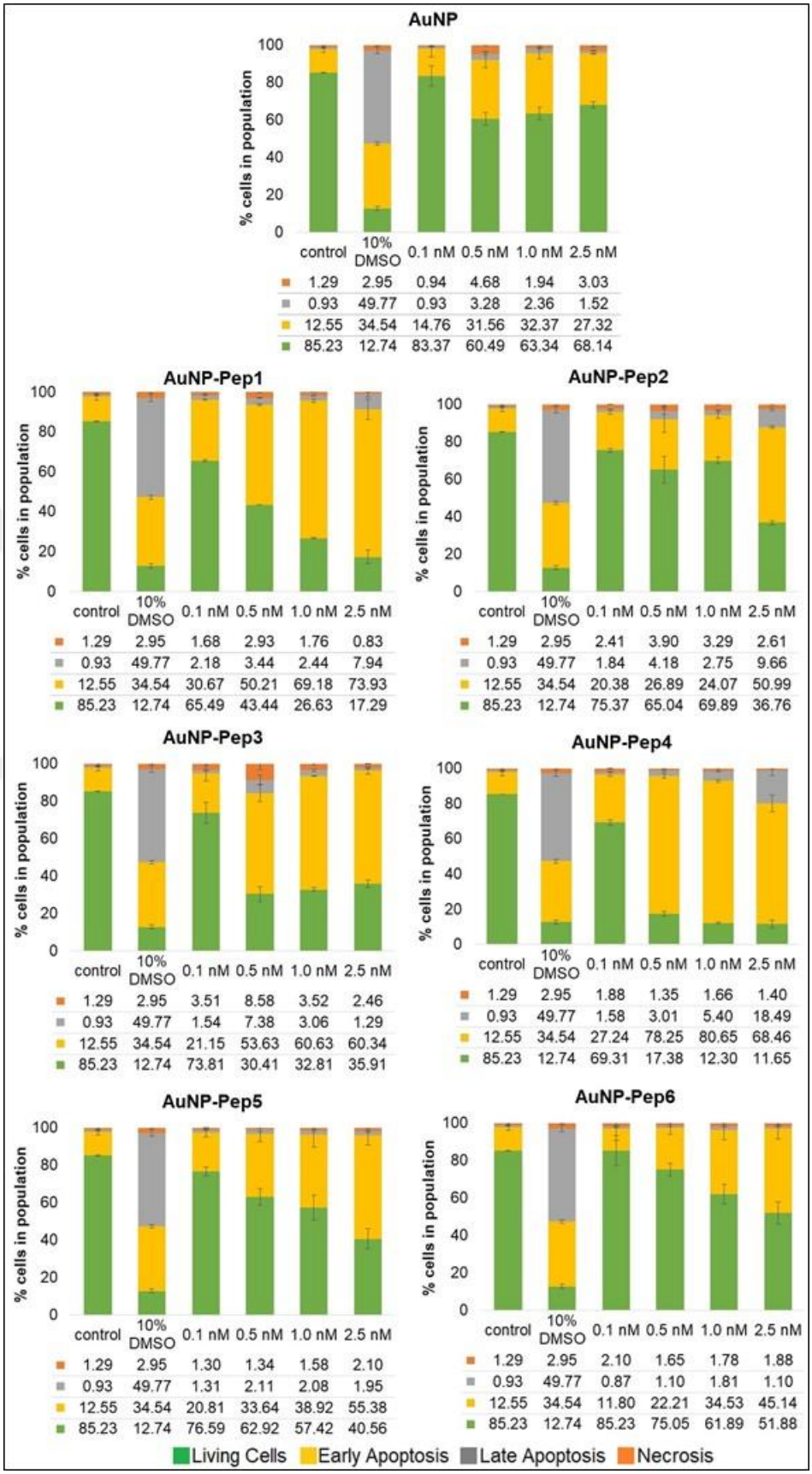

Figure 5.15. Apoptosis-necrosis analysis of DU145 cells.

5.2.2. Cell Cycle

Cell cycle is one of the significant characteristic response of the cells to the active ingredient they exposured. While the any toxic effect is not observed, cell cycle analysis can provide insight into the cellular response. Thus, the cell cycle of the peptide modified AuNP exposured cells was investigated by flow cytometry following the PI staining procedure. PI stains the DNA, thus and so obtaining the life cycle of the cells is became enabled.

The cell replicates its DNA during the life cycle, if do not encounter with any trouble like “cancer”. The phase in which the DNA starts replicating is “S” phase. Here the DNA synthesizing is occurred, which can be mentioned as “preparing” for the G2 phase. In the G2 phase the cell completes the replicates, and finally in M phase the cell have twice as much DNA. Thus, the cell cycle analysis can be investigated by observing the amount of DNA.

In the cell cycle study, 20 000 cells analyzed by flow cytometry were evaluated as 100 per cent of the population. The phases of the cell cycle G0/G1, S, and G2/M ratios were analyzed comparatively.

The cell cycle of the both healthy (PNT1A) and cancer (DU145) cells treated with the bare AuNP and the AuNP-Peptides in increasing concentration was evaluated compatively. 0.1 µM colchicine was used as a positive control. For PNT1A cells, the results are as given in Figure 5.16. The effect of the colchcine is seen as about 90 per cent of the cells in G2/M phase.

There is not significant arrest in G0/G1 phase for the PNT1A except for Pep3 and Pep4 modified AuNPs. For these histidine containing peptides, the treatment results in high G0/G1 ratio as about 70 per cent. Particularly for AuNP-Pep3, which is cysteine C-terminated caused to arrest at G0/G1 phase proportionally with the concentration. Thus, it was investigated that not only the effect of steric hindrance but also the effect of cysteine position in the peptide. On the other hand, cysteine position did not cause significant effect on the cell cyle for the other four peptide pairs. Additionally, Pep5 and Pep6 modified AuNPs indicated less cells in S and G0/G1 phases according to the RGD sequence difference between Pep1-Pep2 and Pep5-Pep6 pairs.

The cell cycle results of the bare AuNP and the peptide modified AuNP exposured DU145 cells are given in Figure 5.17. Herein the higher arrest at G0/G1 phase was obtained for the cysteine N-terminated peptides among the all peptide pairs. Furthermore, 2.5 nM AuNP-Pep5 most effectively arrested the cancer cells at G0/G1 phase.

As a result, while there is no significant arrest at G0/G1 for healthy cells in comparing with control group, the conjugates caused to arrest for cancer cells about 60 per cent.

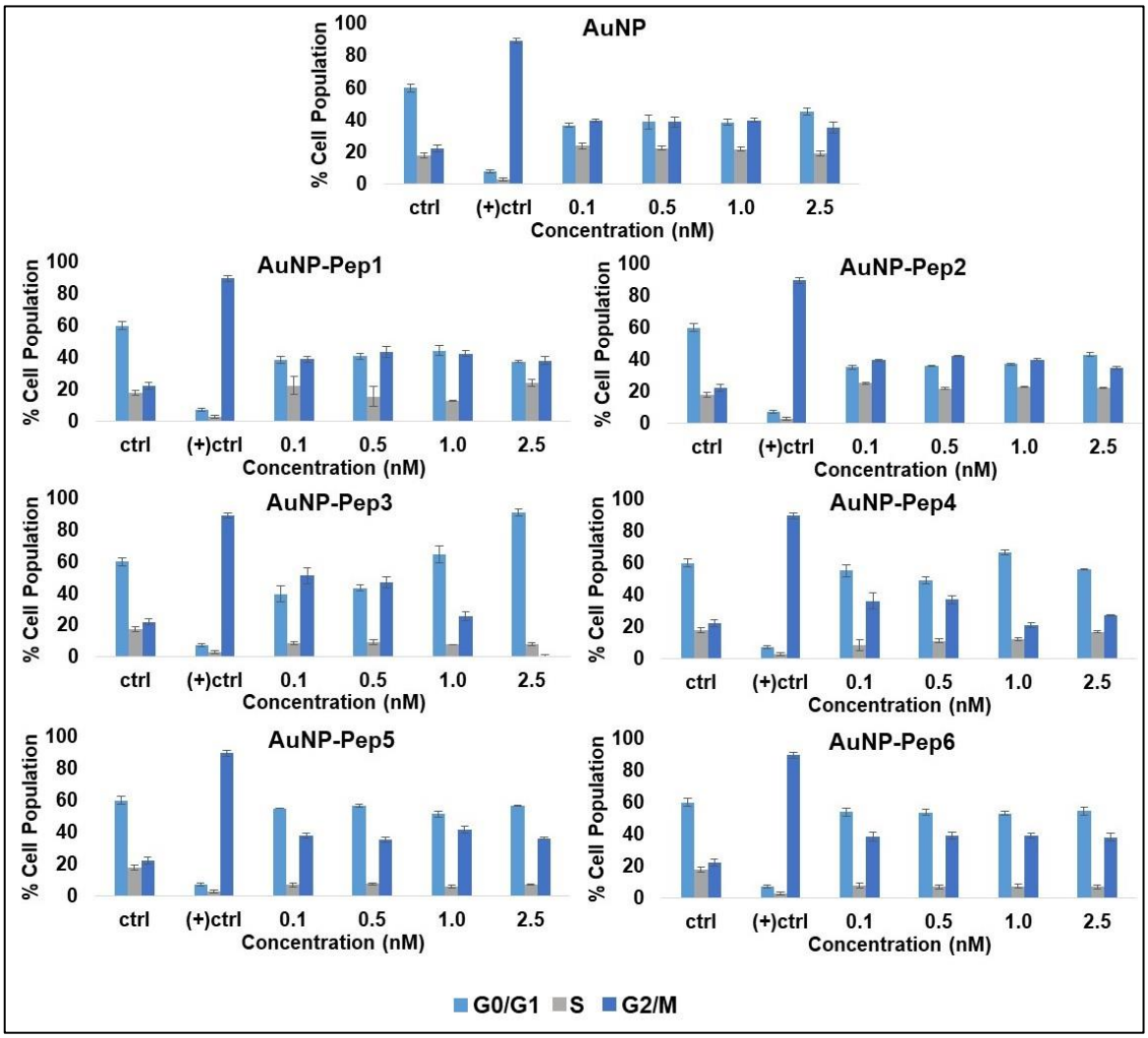

Figure 5.16. Cell cycle analysis of AuNP-Peptide exposed PNT1A cells.

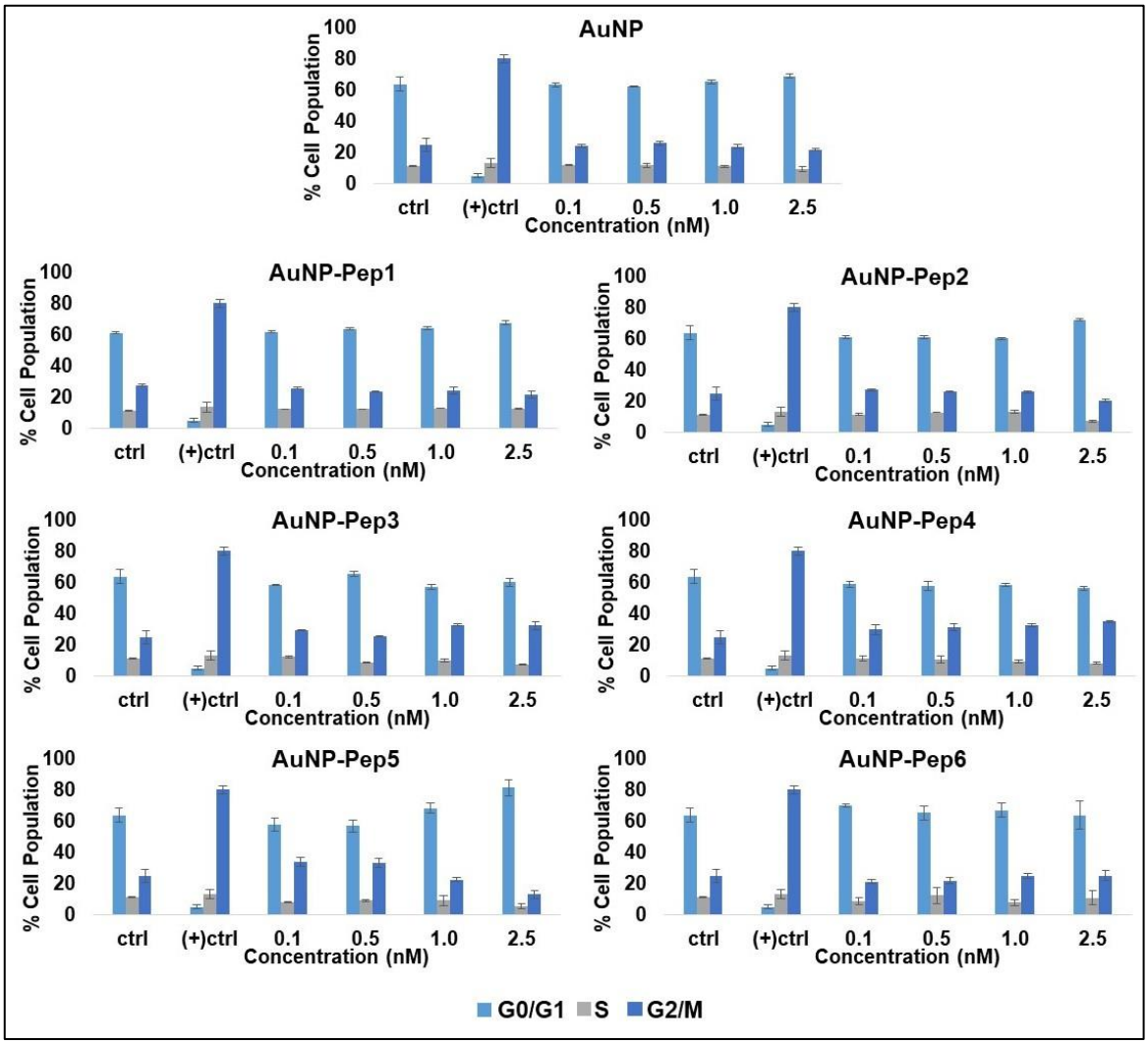

Figure 5.17. Cell cycle analysis of AuNP-Peptide exposed DU145 cells.

6. CONCLUSION AND FUTURE PERSPECTIVE

AuNPs are attractive candidates to be the bricks for nanobiomaterials using in medical fields due to their many distinctive characteristics such as non-toxicity, tunable size, easy surface chemistry, and plasmonic properties. With these features, their behavior in biological media can be altered by functionalization of them with biomolecules. Peptides are the feasible biological modification agents for functionalization of the AuNPs. Their physical and chemical properties such as length, conformation, charge, and hydrophobicity can be tunable by controlling the amino acid sequence.

In this thesis, 13 nm AuNPs were functionalized by the six peptides, which are differ in their sequence, length, and charge by considering needed pH and concentration conditions to obtain the bioconjugation reactions. Hereupon, four of the peptides were four amino acids length, and two of the peptides were seven amino acid length with an RGD motif. The effect of the prepared AuNP-Peptide conjugates was investigated comparatively by treating with both normal (PNT1A) and prostate cancer (DU145) cell lines.

The peptide modified AuNPs showed different toxic effect on both healthy and cancer cell lines depending on the position of Cys amino acid in the peptide sequence. Pep1 (H_2N-Glu-Glu-Glu-Cys-COOH) and Pep5 (H_2N-Asp-Gly-Arg-Glu-Glu-Glu-Cys-COOH) modified AuNPs significantly induced apoptotic cell death for the cancer cell line DU145 compared to the Cys-N-terminal peptide modified AuNPs. On the other hand, Pep3 (H_2N-His-His-His-Cys-COOH) and Pep4 (H_2N-Cys-His-His-His-COOH) functionalized AuNPs caused relatively low apoptosis ratio due to the histidine amino acid, which may caused by cellular uptake capacity and its hydrophobic structure.

In the cell cycle analysis, it was demonstrated that the highest arrest in G0/G1 phase of the healthy cells obtained as 70 per cent with the histidine containing peptide pairs. The pairs also showed significant difference compared to each other due to the Cys position in the sequence. Cys-C-terminal peptide modified AuNPs caused less apoptotic cell death compared to the Cys-N-terminal modified AuNPs. On the other hand, significant apoptosis induction ratio was obtained in the cancer cells for Pep1-Pep2 and Pep5-Pep6 pairs.

In conclusion, it was demonstrated that the small changes on the AuNPs surface depending on sequence of the peptides caused to different cellular responses. While the peptide functionalized AuNPs caused apoptotic cell death in a significant rate, they are non-toxic for the healthy cells. In comparison of the bare AuNP and the AuNP-Peptides, it was indicated that the toxicity level of AuNPs was reduced. In addition, the peptide modified AuNPs caused arrest of DU145 cells at G2/M phase of the cell cycle.

This study indicates the necessity of investigation of surface chemistry effect of nanomaterials to be used in nanomedicine in depth. A range of customized peptides can be used to modify the AuNPs for further investigation. A detailed search using the other advanced techniques including X-ray photoelectron spectroscopy, TEM imaging, and ICP-MS can be conducted as future study. After a detailed study at cellular level including several types of normal and cancerous cell lines is conducted, the study can be extended to *in vivo* to explore the potential terapatic and toxic effects of the nanoparticles with small surface chemistry differences.

REFERENCES

1. Gao W, Liu Z, Li Z. Nano- and microcrystal coatings and their high-temperature applications. *Advanced Materials.* 2001;13:1001–1004.

2. Hoek EMV, Ghosh AK. Nanotechnology-based membranes for water purification. *Nanotechnology Applications for Clean Water*. 2009:47–58.

3. Kharat DK, Muthurajan H, Praveenkumar B. Present and futuristic military applications of nanodevices. *Synthesis and Reactivity in Inorganic, Metal-Organic and Nano-Metal Chemistry.* 2006;36:231–235.

4. Yetisen AK, Qu H, Manbachi A, Butt H, Dokmeci MR, Hinestroza JP, Skorobogatiy M, Khademhosseini A, Yun SH. Nanotechnology in textiles. *ACS Nano.* 2016;10:3042–3068.

5. Wang S, Hou W, Wei L, Jia H, Liu X, Xu B. Antibacterial activity of nano-SiO_2 antibacterial agent grafted on wool surface. *Surface Coating Technology.* 2007;202:460–465.

6. Duncan TV. Applications of nanotechnology in food packaging and food safety: barrier materials, antimicrobials and sensors. *Journal of Colloid and Interface Science.* 2011;363:1–24.

7. Paciotti GF, Kingston DGI, Tamarkin L. Colloidal gold nanoparticles: a novel nanoparticle platform for developing multifunctional tumor-targeted drug delivery vectors. *Drug Development Research.* 2006;67:47–54.

8. Ji AM, Su D, Che O, Li WS, Sun L, Zhang ZY, Yang B, Xu F. Functional gene silencing mediated by chitosan/siRNA nanocomplexes. *Nanotechnology.* 2009;20:405103.

9. Kim H, Achermann M, Balet LP, Hollingsworth JA, Klimov VI. Synthesis and characterization of Co/CdSe core/shell nanocomposites: bifunctional magnetic-optical nanocrystals. *Journal of American Chemical Society.* 2005;127:544–546.

10. Pompa PP, Martiradonna L, Torre AD, Sala FD, Manna L, Vittorio MD, Calabi F, Cingolani R, Rinaldi R. Metal-enhanced fluorescence of colloidal nanocrystals with nanoscale control. *Nature Nanotechnology.* 2006;1:126–130.

11. Pustovalov VK, Babenko VA. Optical properties of gold nanoparticles at laser radiation wavelengths for laser applications in nanotechnology and medicine. *Laser Physics Letters.* 2004;1:516–520.

12. Larson DR, Zipfel WR, Williams RM, Clark SW, Bruchez MP, Wise FW, Webb WW. Water-soluble quantum dots for multiphoton fluorescence imaging in vivo. *Science.* 2003;300:1434–1436.

13. Kim E-M, Jeong H-J. Current status and future direction of nanomedicine: focus on advanced biological and medical applications. *Nuclear Medicine and Molecular Imaging.* 2017;51:106–117.

14. Tiwari PM, Vig K, Dennis VA, Singh SR. Functionalized gold nanoparticles and their biomedical applications. *Nanomaterials.* 2011;1:31–63.

15. Guo S, Huang Y, Jiang Q, et al. Enhanced gene delivery and siRNA silencing by gold nanoparticles coated with charge-reversal polyelectrolyte. *ACS Nano.* 2010;4:5505–5511.

16. Niikura K, Matsunaga T, Suzuki T, Kobayashi S, Yamaguchi H, Orba Y, Kawaguchi A, Hasegawa H, Kajino K, Ninomiya T, Ijiro K, Sawa H. Gold nanoparticles as a vaccine platform: influence of size and shape on immunological responses in vitro and in vivo. *ACS Nano.* 2013;7:3926–3938.

17. 7 Amazing Ways Nanotechnology Is Changing The World. In: Pop. Sci. [cited 2018 21 Jun]. Available from: https://www.popsci.com/science/article/2012-11/7-amazing-ways-nanotechnology-changing-world.

18. Mei Y, Sharma G, Lu Y, Ballauff M, Drechsler M, Irrgang T, Kempe R. High catalytic activity of platinum nanoparticles immobilized on spherical polyelectrolyte brushes. *Langmuir*. 2005;21:12229–12234.

19. Viswanathan S, Narayanan TN, Aran K, et al. Graphene–protein field effect biosensors: glucose sensing. *Materials Today*. 2015;18:513–522.

20. Rogers B, Adams J, Pennathur S. *Nanotechnology: Understanding Small Systems.* Florida: CRC Press; 2017.

21. Sabaeian M, Khaledi-Nasab A. Size-dependent intersubband optical properties of dome-shaped InAs/GaAs quantum dots with wetting layer. *Applied Optics.* 2012;51:4176–4185.

22. Huang H, Tan Z, He Y, Liu J, Sun J, Zhao K, Zhou Z, Tian G, Wong SL, Wee ATS. Competition between hexagonal and tetragonal hexabromobenzene packing on Au(111). *ACS Nano*. 2016;10:3198–3205.

23. Peng S, Cho K. Chemical control of nanotube electronics. *Nanotechnology.* 2000;11:57.

24. Hsiao C-Y, Lin C-H, Hung C-H, Su C-J, Lo Y-R, Lee C-C, Lin H-C, Ko F-H, Huang T-Y, Yang Y-S. Novel poly-silicon nanowire field effect transistor for biosensing application. *Biosensors and Bioelectronics.* 2009;24:1223–1229.

25. O'Connell MJ, Boul P, Ericson LM, Huffman C, Wang Y, Haroz E, Kuper C, Tour J, Ausman KD, Smalley RE. Reversible water-solubilization of single-walled carbon nanotubes by polymer wrapping. *Chemical Physics Letters.* 2001;342:265–271.

26. Ciraci S, Dag S, Yildirim T, Gülseren O, Senger RT. Functionalized carbon nanotubes and device applications. *Journal of Physics Condensed Matter*. 2004;16:R901.

27. Azami M, Rabiee M, Moztarzadeh F. Glutaraldehyde crosslinked gelatin/hydroxyapatite nanocomposite scaffold, engineered via compound techniques. *Polymer Composites* 2010;31:2112–2120.

28. Suhr J, Koratkar N, Keblinski P, Ajayan P. Viscoelasticity in carbon nanotube composites. *Nature Materials.* 2005;4:134–137.

29. Michalet X, Pinaud FF, Bentolila LA, Tsay JM, Doose S, Li JJ, Sundaresan G, Wu AM, Gambhir SS, Weiss S. Quantum dots for live cells, in vivo imaging, and diagnostics. *Science* 2005;307:538–544.

30. Gao X, Cui Y, Levenson RM, Chung LWK, Nie S. In vivo cancer targeting and imaging with semiconductor quantum dots. *Nature Biotechnology.* 2004;22:969–976.

31. Dubertret B, Skourides P, Norris DJ, Noireaux V, Brivanlou AH, Libchaber A. In vivo imaging of quantum dots encapsulated in phospholipid micelles. *Science.* 2002;298:1759–1762.

32. Moghimi SM, Hunter AC, Murray JC. Nanomedicine: current status and future prospects. *The FASEB Journal.* 2005;19:311–330.

33. Pastoriza-Santos I, Liz-Marzán LM. Synthesis of Silver Nanoprisms in DMF. *Nano Letters.* 2002;2:903–905.

34. Métraux GS, Cao YC, Jin R, Mirkin CA. Triangular nanoframes made of gold and silver. *Nano Letters.* 2003;3:519–522.

35. Panáček A, Kvítek L, Prucek R, Kolář M, Večeřová R, Pizúrová N, Sharma VK, Nevěčná T, Zbořil R. Silver colloid nanoparticles: synthesis, characterization, and their antibacterial activity. *The Journal of Physical Chemistry B.* 2006;110:16248–16253.

36. Wiley B, Sun Y, Mayers B, Xia Y. Shape-controlled synthesis of metal nanostructures: the case of silver. *Chemistry a European Journal.* 2004;11:454–463.

37. Shanmukh S, Jones L, Driskell J, Zhao Y, Dluhy R, Tripp RA. Rapid and sensitive detection of respiratory virus molecular signatures using a silver nanorod array sers substrate. *Nano Letters.* 2006;6:2630–2636.

38. Compton D, Cornish L, Lingen E van der. The third order nonlinear optical properties of gold nanoparticles in glasses, part I. *Gold Bulletin.* 2003;36:10–16.

39. Brust M, Walker M, Bethell D, Schiffrin DJ, Whyman R. Synthesis of thiol-derivatised gold nanoparticles in a two-phase liquid–liquid system. *Journal of the Chemical Society, Chemical Communications.* 1994;0:801–802.

40. Aslam M, Fu L, Su M, Vijayamohanan K, Dravid VP. Novel one-step synthesis of amine-stabilized aqueous colloidal gold nanoparticles. *Journal of Materials Chemistry.* 2004;14:1795–1797.

41. Goia DV, Matijević E. Tailoring the particle size of monodispersed colloidal gold. *Colloids and Surfaces A: Physicochemical and Engineering Aspects.* 1999;1-3:139–152.

42. Zhao P, Li N, Astruc D. State of the art in gold nanoparticle synthesis. *Coordination Chemistry Reviews.* 2013;257:638–665.

43. Chen Y, Xianyu Y, Jiang X. Surface modification of gold nanoparticles with small molecules for biochemical analysis. *Accounts of Chemical Research.* 2017;50:310–319.

44. Turkevich J, Stevenson PC, Hillier J. A study of the nucleation and growth processes in the synthesis of colloidal gold. *Discussion of the Faraday Society.* 1951;11:55–75.

45. CBNI News | Centre for Bionano Interactions (CBNI) [cited 2018 25 Jun]. Avaliable from: https://www.ucd.ie/cbni/newsevents/cbni-in-the-news/name,196987,en.html.

46. Huang D, Liao F, Molesa S, Redinger D, Subramanian V. Plastic-compatible low resistance printable gold nanoparticle conductors for flexible electronics. *Journal of the Electrochemical Society.* 2003;150:412–417.

47. Berry CC. Progress in functionalization of magnetic nanoparticles for applications in biomedicine. *Journal of Physics D: Applied Physics.* 2009;42:224003.

48. Sahoo SK, Labhasetwar V. Nanotech approaches to drug delivery and imaging. *Drug Discovery Today.* 2003;8:1112–1120.

49. Kumar A, Ma H, Zhang X, Huang K, Jin S, Liu J, Wei T, Cao W, Zou G, Liang X-J. Gold nanoparticles functionalized with therapeutic and targeted peptides for cancer treatment. *Biomaterials.* 2012;33:1180–1189.

50. de Oliveira Noman L, Sant'Ana AC. The control of the adsorption of bovine serum albumin on mercaptan-modified gold thin films investigated by SERS spectroscopy. *Spectrochimica Acta Part A: Molecular and Biomolecular Spectroscopy.* 2018;204:119–124.

51. Lin WZ, Yeung CY, Liang CK, Huang YH, Liu CC, Hou SY. A colorimetric sensor for the detection of hydrogen peroxide using DNA-modified gold nanoparticles. *Journal of the Taiwan Institue of Chemical Engineers*. 2018;89:49-55.

52. Gukowsky JC, Tan C, Han Z, He L. Cysteamine-modified gold nanoparticles as a colorimetric sensor for the rapid detection of gentamicin. *Journal of Food Science*. 2018;83:1631-1638.

53. Saha K, Agasti SS, Kim C, Li X, Rotello VM. Gold nanoparticles in chemical and biological sensing. *Chemical Reviews.* 2012;112:2739–2779.

54. Maier SA. *Plasmonics: fundamentals and applications*. United States:Springer;2007.

55. Eustis S, El-Sayed MA. Why gold nanoparticles are more precious than pretty gold: noble metal surface plasmon resonance and its enhancement of the radiative and nonradiative properties of nanocrystals of different shapes. *Chemical Society Reviews.* 2006;35:209–217.

56. Kim Y, Johnson RC, Hupp JT. Gold nanoparticle-based sensing of "spectroscopically silent" heavy metal ions. *Nano Letters.* 2001;1:165–167.

57. Huang T, Murray RW. Quenching of [Ru(bpy)3]2+ fluorescence by binding to Au nanoparticles. *Langmuir.* 2002;18:7077–7081.

58. Dyadyusha L, Yin H, Jaiswal S, Brown T, Baumberg JJ, Booy FP, Melvin T. Quenching of CdSe quantum dot emission, a new approach for biosensing. *Chemical Communications.* 2005:3201–3203

59. Kharitonov AB, Shipway AN, Katz E, Willner 1. Gold-nanoparticle/bis-bipyridinium cyclophane-functionalized ion-sensitive field-effect transistors: novel assemblies for sensing of neurotransmitters. *Reviews in Analitical Chemistry.* 2011;18:255–260.

60. Altunbek M, Kuku G, Culha M. Gold nanoparticles in single-cell analysis for surface enhanced raman scattering. *Molecules.* 2016;21:1617.

61. Huang X, El-Sayed IH, Qian W, El-Sayed MA. Cancer cell imaging and photothermal therapy in the near-infrared region by using gold nanorods. *Journal of American Chemical Society*. 2006;128:2115–2120.

62. Elghanian R, Storhoff JJ, Mucic RC, Letsinger RL, Mirkin CA. Selective colorimetric detection of polynucleotides based on the distance-dependent optical properties of gold nanoparticles. *Science.* 1997;277:1078–1081.

63. Mirkin CA, Letsinger RL, Mucic RC, Storhoff JJ. A DNA-based method for rationally assembling nanoparticles into macroscopic materials. *Nature.* 1996;382:607–609.

64. Otsuka H, Akiyama Y, Nagasaki Y, Kataoka K. Quantitative and reversible lectin-induced association of gold nanoparticles modified with alpha-lactosyl-omega-mercapto-poly(ethylene glycol). *Journal of American Chemical Society* 2001;123:8226–8230.

65. Yang W, Gooding JJ, He Z, Li Q, Chen G. Fast colorimetric detection of copper ions using L-cysteine functionalized gold nanoparticles. *Journal of Nanoscience and Nanotechnology*. 2007;7:712–716.

66. Thaxton CS, Georganopoulou DG, Mirkin CA. Gold nanoparticle probes for the detection of nucleic acid targets. *Clinica Chimica Acta International Journal of Clinical Chemistry*. 2006;363:120–126.

67. Lin J-H, Zhang L-J, Zhang H, Zhang S-S. Amperometric immunosensor for prostate specific antigen based on co-adsorption of labeled antibody and mediator in nano-au modified chitosan membrane. *Chinese Journal of Chemistry.* 2008;26:480–484.

68. Tsoli M, Kuhn H, Brandau W, Esche H, Schmid G. Cellular uptake and toxicity of Au_{55} clusters. *Small.* 2005;1:841-844.

69. Dutta D, Sundaram SK, Gary J, Brian T, Riley J, Fifield LS, Jacobs JM, Addleman SR, Kaysen GA, Moudgil BM, Weber TJ. Adsorbed proteins influence the biological activity and molecular targeting of nanomaterials. *Toxicological Sciences*. 2007;100:303–315.

70. Hussain SM, Braydich-Stolle LK, Schrand AM, Murdock RC, Yu KO, Mattie DM, Schlager JJ, Terrones M. Toxicity evaluation for safe use of nanomaterials: recent achievements and technical challenges. *Advanced Materials.* 2009;21:1549-1559.

71. Sayes CM, Wahi R, Kurian PA, Liu Y, West JL, Ausman KD, Warheit DB, Colvin VL. Correlating nanoscale titania structure with toxicity: a cytotoxicity and inflammatory response study with human dermal fibroblasts and human lung epithelial cells. *Toxicological Sciences*, 2006;92:174–185.

72. DeLong RK, Reynolds CM, Malcolm Y, Schaeffer A, Severs T, Wanekaya A. Functionalized gold nanoparticles for the binding, stabilization, and delivery of therapeutic DNA, RNA, and other biological macromolecules. *Nanotechnology Science and Applications*. 2010;3:53–63.

73. Moghimi SM, Szebeni J. Stealth liposomes and long circulating nanoparticles: critical issues in pharmacokinetics, opsonization and protein-binding properties. *Progress in Lipid Research.* 2003;42:463–478.

74. Mu Q, Kievit FM, Kant RJ, Lin G, Jeon M, Zhang M. Anti-HER2/neu peptide-conjugated iron oxide nanoparticles for targeted delivery of paclitaxel to breast cancer cells. *Nanoscale.* 2015;7:18010–18014.

75. Song C, Zhong Y, Jiang X, Peng F, Lu Y, Ji X, Su Y, He Y. Peptide-conjugated fluorescent silicon nanoparticles enabling simultaneous tracking and specific destruction of cancer cells. *Analitical Chemistry.* 2015;87:6718–6723.

76. Meziani MJ, Sun Y-P. Protein-conjugated nanoparticles from rapid expansion of supercritical fluid solution into aqueous solution. *Journal of American Chemical Society.* 2003;125:8015–8018.

77. Lemarchand C, Gref R, Couvreur P. Polysaccharide-decorated nanoparticles. *European Journal of Pharmaceutics and Biopharmaeutics.* 2004;58:327–341.

78. Csáki A, Kaplanek P, Möller R, Fritzsche W. The optical detection of individual DNA-conjugated gold nanoparticle labels after metal enhancement. *Nanotechnology.* 2003;14:1262.

79. Dunn SS, Tian S, Blake S, Wang J, Galloway AL, Murphy A, Pohlhaus PD, Rolland JP, Napier ME, DeSimone JM. Reductively responsive sirna-conjugated hydrogel nanoparticles for gene silencing. *Journal of American Chemical Society.* 2012;134:7423–7430.

80. Arruebo M, Valladares M, González-Fernández Á. Antibody-conjugated nanoparticles for biomedical applications. *Journal of Nanomaterials.* 2009;37:1–37:24.

81. Arosio D, Manzoni L, Araldi EMV, Scolastico C. Cyclic RGD functionalized gold nanoparticles for tumor targeting. *Bioconjugate Chemistry.* 2011;22:664–672.

82. Sperling RA, Parak WJ. Surface modification, functionalization and bioconjugation of colloidal inorganic nanoparticles. *Physical and Engineering Sciences.* 2010;368:1333–1383.

83. Alex S, Tiwari A. Functionalized gold nanoparticles: synthesis, properties and applications-a review. *Journal of Nanoscience and Nanotechnology.* 2015;15:1869–1894.

84. Chen W, He S, Pan W, Jin Y, Zhang W, Jiang X. Strategy for the modification of electrospun fibers that allows diverse functional groups for biomolecular entrapment. *Chemical Materials.* 2010;22:6212–6214.

85. Sonawane MD, Nimse SB. Surface modification chemistries of materials used in diagnostic platforms with biomolecules. *Journal of Chemistry.* 2016;9241378.

86. Hermanson GT. *Bioconjugate Techniques.* United Kingdom:Academic Press;2013.

87. Pow DV, Crook DK. Extremely high titre polyclonal antisera against small neurotransmitter molecules: rapid production, characterisation and use in lightand electron-microscopic immunocytochemistry. *Journal of Neuroscience Methods.* 1993;48:51–63.

88. Nicol JR, Dixon D, Coulter JA. Gold nanoparticle surface functionalization: a necessary requirement in the development of novel nanotherapeutics. *Nanomedicine.* 2015;10:1315–1326.

89. Ye X, Jin L, Caglayan H, et al. Improved size-tunable synthesis of monodisperse gold nanorods through the use of aromatic additives. *ACS Nano.* 2012;6:2804–2817.

90. Cho W-S, Cho M, Jeong J, Choi M, Han BS, Shin H-S, Hong J, Chung BH, Jeong J, Cho M-H. Size-dependent tissue kinetics of PEG-coated gold nanoparticles. *Toxicology and Applied Pharmacology.* 2010;245:116–123.

91. Kumar D, Meenan BJ, Dixon D. Glutathione-mediated release of Bodipy® from PEG cofunctionalized gold nanoparticles. *International Journal of Nanomedicine.* 2012;7:4007–4022.

92. Slocik JM, Govorov AO, Naik RR. Plasmonic circular dichroism of peptide-functionalized gold nanoparticles. *Nano Letters.* 2011;11:701–705.

93. Tsai D-H, Cho TJ, Elzey SR, Gigault JC, Hackley VA. Quantitative analysis of dendron-conjugated cisplatin-complexed gold nanoparticles using scanning particle mobility mass spectrometry. *Nanoscale.* 2013;5:5390–5395.

94. Jazayeri MH, Amani H, Pourfatollah AA, Pazoki-Toroudi H, Sedighimoghaddam B. Various methods of gold nanoparticles (GNPs) conjugation to antibodies. *Sensing and Bio-Sensing Research.* 2016;9:17–22.

95. Kumar S, Aaron J, Sokolov K. Directional conjugation of antibodies to nanoparticles for synthesis of multiplexed optical contrast agents with both delivery and targeting moieties. *Nature Protocols.* 2008;3:314–320.

96. Rayavarapu RG, Petersen W, Ungureanu C, Post JN, van Leeuwen TG, Manohar S. Synthesis and bioconjugation of gold nanoparticles as potential molecular probes for light-based imaging techniques. *International Journal of Biomedical Imaging* 2007;29817.

97. Zhang Z, Wang S, Xu H, Wang B, Yao C. Role of 5-aminolevulinic acid-conjugated gold nanoparticles for photodynamic therapy of cancer. *Journal of Biomedical Optics* 2015;20:51043.

98. El-Sayed IH, Huang X, El-Sayed MA. Surface plasmon resonance scattering and absorption of anti-EGFR antibody conjugated gold nanoparticles in cancer diagnostics: applications in oral cancer. *Nano Letters* 2005;5:829–834.

99. Sumbayev VV, Yasinska IM, Garcia CP, Gilliland D, Lall GS, Gibbs BF, Bonsall DR, Varani L, Rossi F, Calzolai L. Gold nanoparticles downregulate interleukin-1β-induced pro-inflammatory responses. *Small.* 2012;9:472–477.

100. Werengowska-Ciećwierz K, Wiśniewski M, Terzyk AP, Furmaniak S. (2015) The chemistry of bioconjugation in nanoparticles-based drug delivery system. *Advances in Condensed Matter Physics*. 2015;198175.

101. Ljungblad J. Antibody-conjugated gold nanoparticles integrated in a fluorescence based biochip. 2009.

102. Yu MK, Park J, Jon S. Targeting strategies for multifunctional nanoparticles in cancer imaging and therapy. *Theranostics.* 2012;2:3–44.

103. Wu RH, Nguyen TP, Marquart GW, Miesen TJ, Mau T, Mackiewicz MR. A facile route to tailoring peptide-stabilized gold nanoparticles using glutathione as a synthon. *Molecules.* 2014;19:6754–6775.

104. Arkan E, Saber R, Karimi Z, Mostafaie A, Shamsipur M. Multiwall carbon nanotube-ionic liquid electrode modified with gold nanoparticles as a base for preparation of a novel impedimetric immunosensor for low level detection of human serum albumin in biological fluids. *Journal of Pharmaceutical and Biomedical Analysis.* 2014;92:74–81.

105. Chen J, Saeki F, Wiley BJ, et al. Gold nanocages: bioconjugation and their potential use as optical imaging contrast agents. *Nano Letters.* 2005;5:473–477.

106. Singh V, Nair SPN, Aradhyam GK. Chemistry of conjugation to gold nanoparticles affects G-protein activity differently. *Journal of Nanobiotechnology.* 2013;11:7.

107. Di Pasqua AJ, Mishler RE, Ship Y-L, Dabrowiak JC, Asefa T. Preparation of antibody-conjugated gold nanoparticles. *Material Letters.* 2009;63:1876–1879.

108. Dam DHM, Lee H, Lee RC, Kim KH, Kelleher NL, Odom TW. Tunable loading of oligonucleotides with secondary structure on gold nanoparticles through a pH-driven method. *Bioconjugation Chemistry.* 2015;26:279–285.

109. Sharma N, Top A, Kiick KL, Pochan DJ. One-dimensional gold nanoparticle arrays by electrostatically directed organization using polypeptide self-assembly. *Angewandte Chemie International Edition.* 2009;48:7078–7082.

110. Kingston DGI, Cao S, Zhao J, Paciotti GF, Hubta MS. Thiolated paclitaxels for reaction with gold nanoparticles as drug delivery agents. U.S. Patent No 8,558,019, 2013.

111. Krpetić Ž, Nativo P, Porta F, Brust M. A multidentate peptide for stabilization and facile bioconjugation of gold nanoparticles. *Bioconjugate Chemistry.* 2009;20:619–624.

112. Aili D, Enander K, Rydberg J, Lundström I, Baltzer L, Liedberg B. Aggregation-induced folding of a de novo designed polypeptide immobilized on gold nanoparticles. *Journal of American Chemical Society.* 2006;128:2194–2195.

113. Kim J, Sadowsky MJ, Hur H-G. Simultaneous synthesis of temperature-tunable peptide and gold nanoparticle hybrid spheres. *Biomacromolecules.* 2011;12:2518–2523.

114. Norde W. Adsorption of proteins from solution at the solid-liquid interface. *Advances in Colloid and Interface Science.* 1986;25:267–340.

115. Geoghegan WD. The effect of three variables on adsorption of rabbit IgG to colloidal gold. *Journal of Histochemistry and Cytochemistry.* 1988;36:401–407.

116. Tokuyasu KT. Present state of immunocryoultramicrotomy. *Journal of Histochemistry and Cytochemistry Official Journal of the Histochemical Society.* 1983;31:164–167.

117. Tinglu G, Ghosh A, Ghosh BK. Subcellular localization of alkaline phosphatase in Bacillus licheniformis 749/C by immunoelectron microscopy with colloidal gold. *Journal of Bacteriology.* 1984;159:668–677

118. Horisberger M, Clerc M-F. Labelling of colloidal gold with protein A. *Histochemistry.* 1985;82:219–223

119. Ackerman, Forrest J. Male Prostate Anatomy [cited 2018 30 Jun]. Available from: http://libcat.org//male-prostate-anatomy.

120. Garraway M. *Epidemiology of Prostate Disease.* Berlin Heidelberg:Springer-Verlag Press;1995.

121. Taylor BS, Schultz N, Hieronymus H, et al. Integrative genomic profiling of human prostate cancer. *Cancer Cell.* 2010;18:11–22.

122. Gann PH. Risk factors for prostate cancer. *Reviews in Urology*. 2002;4:3–10.

123. Cancer Facts & Figures 2016 | American Cancer Society [cited 2018 28 Jun]. Available from: https://www.cancer.org/research/cancer-facts-statistics/.

124. Cuzick J, Thorat MA, Andriole G, et al. Prevention and early detection of prostate cancer. *The Lancet Oncology.* 2014;15:484–492.

125. Prostate Cancer Treatment. In: Natl. Cancer Inst. [cited 2018 Jun 28]. Available from: https://www.cancer.gov/types/prostate/patient/prostate-treatment-pdq.

126. Johnson DH. Targeted therapies in combination with chemotherapy in non-small cell lung cancer. *Clinical Cancer Research an Official Journal of the American Association for Cancer Research.* 2006;12:4451–4457.

127. Peschel RE, Colberg JW. Surgery, brachytherapy, and external-beam radiotherapy for early prostate cancer. *The Lancet Oncology.* 2003;4:233–241.

128. Ojima I, Lichtenthal B, Lee S, Wang C, Wang X. Taxane anticancer agents: a patent perspective. *Expert Opinion on Therapeutic Patents.* 2016;26:1–20.

129. Baisden BL, Kahane H, Epstein JI. Perineural invasion, mucinous fibroplasia, and glomerulations: diagnostic features of limited cancer on prostate needle biopsy. *The American Journal of Surgical Pathology.* 1999;23:918.

130. Lilja H, Ulmert D, Vickers AJ. Prostate-specific antigen and prostate cancer: prediction, detection and monitoring. *Nature Reviews Cancer.* 2008;8:268–278.

131. Chen Z, Penet M-F, Nimmagadda S, Li C, Banerjee SR, Winnard PT, Artemov D, Glunde K, Pomper MG, Bhujwalla ZM. PSMA-targeted theranostic nanoplex for prostate cancer therapy. *ACS Nano.* 2012;6:7752–7762.

132. Melancon MP, Stafford RJ, Li C. Challenges to effective cancer nanotheranostics. *Journal of Controlled Release.* 2012;164:177–182.

133. Adhami VM, Malik A, Zaman N, Sarfaraz S, Siddiqui IA, Syed DN, Afaq F, Pasha FS, Saleem M, Mukhtar H. Combined inhibitory effects of green tea polyphenols and selective cyclooxygenase-2 inhibitors on the growth of human prostate cancer cells both in vitro and in vivo. *Clinical Cancer Research.* 2007;13:1611–1619.

134. K. Nune S, Chanda N, Shukla R, Katti K, R. Kulkarni R, Thilakavathy S, Mekapothula S, Kannan R, V. Katti K. Green nanotechnology from tea: phytochemicals in tea as building blocks for production of biocompatible gold nanoparticles. *Journal of Materials Chemistry.* 2009;19:2912–2920.

135. Teiten M-H, Gaascht F, Eifes S, Dicato M, Diederich M. Chemopreventive potential of curcumin in prostate cancer. *Genes & Nutrition.* 2010;5:61.

136. Mukerjee A, Vishwanatha JK. Formulation, characterization and evaluation of curcumin-loaded PLGA nanospheres for cancer therapy. *Anticancer Research.* 2009;29:3867–3875.

137. Syrovets T, Gschwend JE, Büchele B, Laumonnier Y, Zugmaier W, Genze F, Simmet T. Inhibition of IκB kinase activity by actyl-boswellic acids promotes apoptosis in androgen-independent PC-3 prostate cancer cells in vitro and in vivo. *Journal of Biological Chemistry*. 2004;280:6170-6180.

138.Uthaman S, Snima KS, Annapoorna M, Ravindranath KC, Shanti V, Lakshmanan V-K. Novel boswellic acids nanoparticles induces cell death in prostate cancer cells. *Journal of Natural Products.* 2012;5:100–108.

139.Aggarwal S, Singh P, Topaloglu O, Isaacs JT, Denmeade SR. A dimeric peptide that binds selectively to prostate-specific membrane antigen and inhibits its enzymatic activity. *Cancer Research.* 2006;66:9171–9177.

140.Kim D, Jeong YY, Jon S. A drug-loaded aptamer−gold nanoparticle bioconjugate for combined CT imaging and therapy of prostate cancer. *ACS Nano* 2010;4:3689–3696.

141.Lewin M, Carlesso N, Tung CH, Tang XW, Cory D, Scadden DT, Weissleder R. Tat peptide-derivatized magnetic nanoparticles allow in vivo tracking and recovery of progenitor cells. *Nature Biotechnology.* 2000;18:410–414.

142.Zhao M, Kircher MF, Josephson L, Weissleder R. Differential conjugation of tat peptide to superparamagnetic nanoparticles and its effect on cellular uptake. *Bioconjugate Chemistry.* 2002;13:840–844.

143.Frens G. Controlled nucleation for the regulation of the particle size in monodisperse gold suspensions. *Nature Physical Science.* 1973;241:20-22.

144.Basu S, Ghosh SK, Kundu S, Panigrahi S, Praharaj S, Pande S, Jana S, Pal T. Biomolecule induced nanoparticle aggregation: effect of particle size on interparticle coupling. *Journal of Colloid and Interface Science.* 2007;313:724–734.

145.Kainth S, Basu S. Quantitative detection of thiopurines by inter-particle distance-dependent properties of gold nanoparticles. *Plasmonics.* 2018;1–9.

146.Suchomel P, Kvitek L, Prucek R, Panacek A, Halder A, Vajda S, Zboril R. Simple size-controlled synthesis of Au nanoparticles and their size-dependent catalytic activity. *Scientific Reports.* 2018;8:4589.

147.Basu S, Pande S, Jana S, Bolisetty S, Pal T. Controlled interparticle spacing for surface-modified gold nanoparticle aggregates. *Langmuir.* 2008;24:5562–5568.

148. Shao X, Schnau P, Qian W, Wang X. Quantitatively understanding cellular uptake of gold nanoparticles via radioactivity analysis. *Journal of Nanoscience and Nanotechnology*. 2015;15:3834–3838.

149. Roma-Rodrigues C, Heuer-Jungemann A, Fernandes AR, Kanaras AG, Baptista PV. Peptide-coated gold nanoparticles for modulation of angiogenesis in vivo. *International Journal of Nanomedicine.* 2016;11:2633–2639.

150. Murdock RC, Braydich-Stolle L, Schrand AM, Schlager JJ, Hussain SM. Characterization of nanomaterial dispersion in solution prior to in vitro exposure using dynamic light scattering technique. *Toxicological Sciences: an Official Journal of the Society of Toxicology.* 2008;101:239–253.

151. Neuberger T, Schöpf B, Hofmann H, Hofmann M, von Rechenberg B. Superparamagnetic nanoparticles for biomedical applications: possibilities and limitations of a new drug delivery system. *Journal of Magnetism and Magnetic Materials.* 2005;293:483–496.

152. Hanauer M, Pierrat S, Zins I, Lotz A, Sönnichsen C. Separation of nanoparticles by gel electrophoresis according to size and shape. *Nano Letters*. 2007;7:2881–2885.

153. Sperling RA, Pellegrino T, Li JK, Chang WH, Parak WJ. Electrophoretic separation of nanoparticles with a discrete number of functional groups. *Advanced Functional Materials*. 2006;16:943–948.

154. Rodrigues L, Mota M. *Bioinspired materials for medical applications.* Braga: Elsevier; 2017.

155. Xia Z, Wang P, Liu X, Liu T, Yan Y, Yan J, Zhong J, Sun G, He D. Tumor-penetrating peptide-modified DNA tetrahedron for targeting drug delivery. *Biochemistry*. 2016;55:1326–1331.